NOTICE

The quality of this microform is heavily dependent upon the quality of the original thesis submitted for microfilming. Every effort has been made to ensure the highest quality of reproduction possible.

If pages are missing, contact the university which granted the degree.

Some pages may have indistinct print especially if the original pages were typed with a poor typewriter ribbon or if the university sent us an inferior photocopy.

Previously copyrighted materials (journal articles, published tests, etc.) are not filmed.

Reproduction in full or in part of this microform is governed by the Canadian Copyright Act, R.S.C. 1970, c. C-30.

AVIS

La qualité de cette microforme dépend grandement de la qualité de la thèse soumise au microfilmage. Nous avons tout fait pour assurer une qualité supérieure de reproduction.

S'il manque des pages, veuillez communiquer avec l'université qui a conféré le grade.

La qualité d'impression de certaines pages peut laisser à désirer, surtout si les pages originales ont été dactylographiées à l'aide d'un ruban usé ou si l'université nous a fait parvenir une photocopie de qualité inférieure.

Les documents qui font déjà l'objet d'un droit d'auteur (articles de revue, tests publiés, etc.) ne sont pas microfilmés.

La reproduction, même partielle, de cette microforme est soumise à la Loi canadienne sur le droit d'auteur, SRC 1970, c. C-30.

Target Theory

Mousa Mohammad-Nazhad

A Thesis

in

The Department

of

Physics

Presented in Partial Fulfillment of the Requirements for the Degree of Master of Science at Concordia University
Montréal, Québec, Canada

August 1987

ISBN 0-315-41636-X

ABSTRACT

Target Theory

M.M.Nazhad

Previous estimates of energy deposition by ionizing particles in biological systems have generally been made through considering energy deposited by track core or taking into account the delta rays in the concept of averaged dose. There has been considerable disagreement in the interpretation of the results of these works.

Today, more precise analysis has become available with the development of the Monte Carlo method of simulating the tracks of charged particles event by event (10).

In this work, the development of target theory up to the work of Katz (9) and Paretzke (10) has been studied. Their two approaches which are different from each other, are investigated and compared. This is done by calculating the inactivation cross-section versus LET, following Paretzke's approach and comparing the results to those obtained by Katz.

ACKNOWLEDGEMENTS

The author wishes to express his appreciation to Dr. D. E. Charlton for his valuable advice and constant interest throughout this investigation.

The author is deeply grateful to professors S. K. Misra and C. K. Kalman for their help in providing facilities during the course of the work.

The author is also indepted to Dr. N. W. Eddy and Dr. C. Eappen for their kindness and continued encouragement.

The author would like to acknowledge the teaching assistantship received from the Physics Department.

Finally, the author wishes to record his appreciation to his wife Taiebeh, and son Arash for their patience and help during the study.

TABLES OF CONTENTS

LIST OF FIGURES

LIST OF TABLES

CHAPTER I

INTRODUCTION AND SURVEY

1.1 General

Once philosophy included all arts and sciences. It was actualy regarded as the science of all sciences. However, from the renaissance the different disciplines began to develop independently, and this trend has continued up to the present time.

Today we witness the mutual influence of the different branches of science. Biology, for instance, is contributing to the science of organic chemistry to find answers to the many questions which the latter has encountered.

When in 1933, Stanly produced paracrystals of tobacco-mosaic viruses and Heisenberg, Einstein,, and Dirac redirected the course of physics, biology and physics met each other again. From that time onwards physics began to be applied increasingly in biology. Examples include: the study of the cell damage processes, radiosensitivity of materials, determination of shape and structure of biological systems.

This meeting of the two sciences has produced very important results, not least the establishment of radiobiological dosimetry as a discipline in its own right.

1.2 Introduction of Target Theory

Pioneers in the application of ionizing radiation in solutions are Hussey and Thompson(1), and Northrop(2). They bombarded enzymes in solution with x-rays, but their attempt to correlate a given dose to the inactivation of the enzymes failed. The reason for this failure was that the activation of the water was responsible for the destruction of the enzyme. This was confirmed by Fricke(3) who irradiated enzymes in dry state. In 1939, Svedberg and Brohult (3a) repeated the experiments of Hussey and Northrop this time with alpha rays instead of x-rays. The results showed a correlation between dose and inactivation, because alpha rays do not generate considerable activation of water(5b).

From these beginnings Lea (4b) then established the concept of "Target Theory ". In a classic paper Lea assessed the effect of x-rays on dried enzymes (myosin and ribonuclease) and determined the inactivation volume. He used dried enzymes to eliminate the indirect effect of water. This work led to the establishment of " Target Theory " based on the following principles :

1) One or more primary ionizations anywhere within an enzyme molecule are sufficient to inactivate it.

2) The ionizations outside the molecule do not affect enzymes activity

3) Excitation is not significant for inactivation process.

Pollard (5c), then tried to develop Lea's studies by applying radiation on different biological systems. He confirmed the relationship between the radiosensitivity and

the molecular weight of biological molecules, and used this method to calculate molecular weights. However, the lack of precision of these results, led Pollard and his collaborators to attempt unsuccessfully, a correction of Target Theory.

1.2.1 Problems in Target Theory

Brustad (6) in 1961 determined the deposited energy versus inactivation cross-section for trypsin, lysozyme, and ribonuclease by irradiation with protons, carbon and neon ions. The result were surprising, for example, the effect of protons on the enzymes with LET 3.6keV/micrometer was 65 times that of neon with LET=450keV/ micrometer, thus lower radiation energy caused greater inactivation. Furthermore, following Alexander and Charlesby (7), Brustad investigated the effect of irradiation on mixtures of trypsin and lactose, and showed that molecular interaction had significant role in radiation inactivation.

The importance of these experiments was to identify the problems to be solved in Target Theory. With Dolphin and Hutchinson (8), Brustad tried to solve these problems with a " delta-ray correction " approach. Both Katz et al (9) and Paretzke (10) refined this approach by pinpointing the importance of " Track Structure ". This takes into account the many delta-rays produced whose path is transvers to the ion's path, generating a " delta-ray cloud ".

However, their approaches, as will be shown have important

differences. Generally speaking, Katz's method obtains good results for enzymes and viruses irradiated with heavy charged particles, but it is less successful in other cases. Paretzke has shown that Katz's concept of " Average Dose " has serious shortcomings. He argues that the stochastic nature of " energy deposition " cannot be ignored and that there is a great deal of research left to do before the effects of track structure can be accurately formulated. " Target Theory " has been very productive, and many questions have been answered, but of course, in the process many new questions have arisen.

" There is no royal path to science "

1.3 The Aims of the Thesis

In this paper the development of target theory up to the work of Katz and Paretzke isundertaken. Their two approaches are investigated and compared to each other. This is done by calculating the inactivation cross-section versus LET, following Paretzke's approach and comparing the results to those obtained by Katz.

We begin with a survey of ionizing radiation (i.e. x-,gamma-rays, alpha and beta particles). This is followed by a discussion of primary and secondary ionization and the Bragg peak. We then proceed to an investigation of the concept of stopping power. This will logically lead to the introduction of " Linear Energy Transfer ". The analysis of dosimetry, microdosimetry, and the relationship between

dose, kerma, and exposure will provide the subject matter of Chapter III. Target Theory which is the focal point of this thesis will be extensively studied in Chapter IV. There we will also discuss the calculation of the molecular size of some large molecules.

Chapter V begins with the alternative approaches to target theory initiated by Katz and Paretzke. This is followed by the calculation of inactivation cross-section versus LET based on Paretzke's work using data provided by Charlton (11). We conclude with a comparison of these results with those obtained by Katz.

CHAPTER II

THE BACKGROUND OF IONIZING RADIATION

2.1 Introduction

Historically it was mentioned that some minerals continually give off certain typesof radiations which were named alpha, beta and gamma radiations, whose nature was later discovered. The alpha-particle was identified with helium nuclei, the beta-particle with electrons, and gamma-rays with quanta of electromagnetic radiation. The particles which have been most used as ionizing radiations in biological study are either uncharged or lightly charged particles(fully stripped U atoms have been used). In the following several different types of radiations are discussed.

2.2 Discovery of X-rays

X-rays were discovered by Roentgen in 1895. He showed that these X-rays, as Roentgen called them, had very great penetrating power. It was also found these rays could blacken a photographic plate and could ionize a gas. The X-rays travelled in straight lines from the source and were not deflected in passing through electric and magnetic fields. They were thus not charged particles. The wave nature of x-rays was definitly established by Laue's experiments on the diffraction of x-rays by crystals (1912).

With a knowledge of the grating space of a crystal and the use of the Bragg equation, it was possible to measure the wave lengths of the x-rays emitted by the target of an x-ray tube. By means of a crystal spectrometer, it was found that x-rays consist of two distinct types of spectra, 1) Continuous x-ray 2) characteristic x-ray

2.2.1 Continuous x-rays

Let us consider that a fast moving electron aproaches the nucleus of an atom. In this case the electron experiences a large amount of attractive force. This causes deflection of the electron from its path. The deflected electron radiates one or more photons. This radiation is called continuous x-ray or bremsstrahlung. This is demonstrated by figure(2.1).

2.2.2 Characteristic x-rays

A typical x-ray spectrum, obtained by Ulrey (12) is shown in the curves in Fig.(2.2) in which the intensity of the x-rays plotted against wavelength. The curves for tungsten show the continuous spectrum of the x-rays at a voltage of 35 kV. The curve for molybdenum was obtained under similar conditions and shows two sharp lines characteristic of the molybdenum superimposed on the continuous spectrum. These lines are called as the k_α and k_β lines of molybdenum. This monoenergetic radiations can be explained by the electron configurations of the atoms.

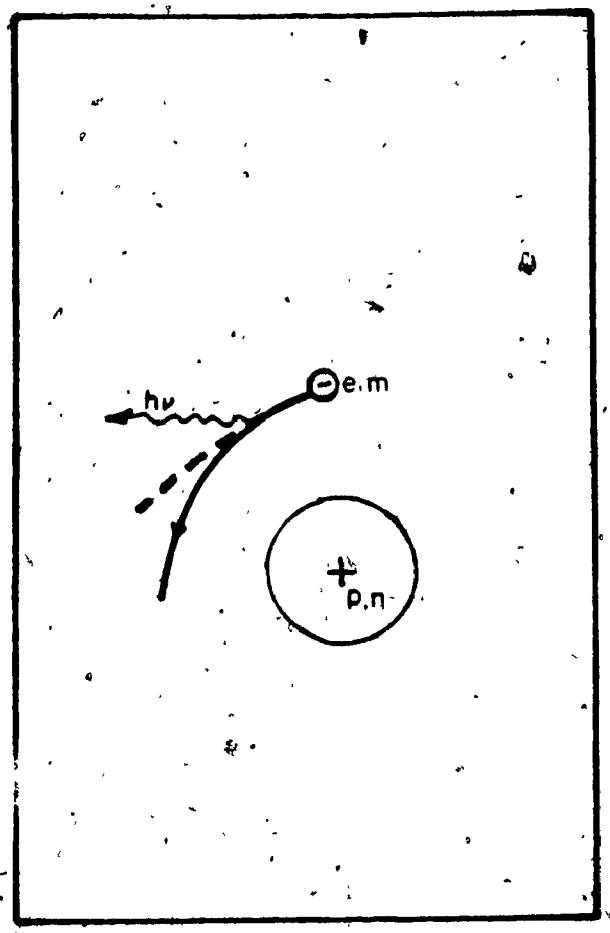

Fig.(2.1)

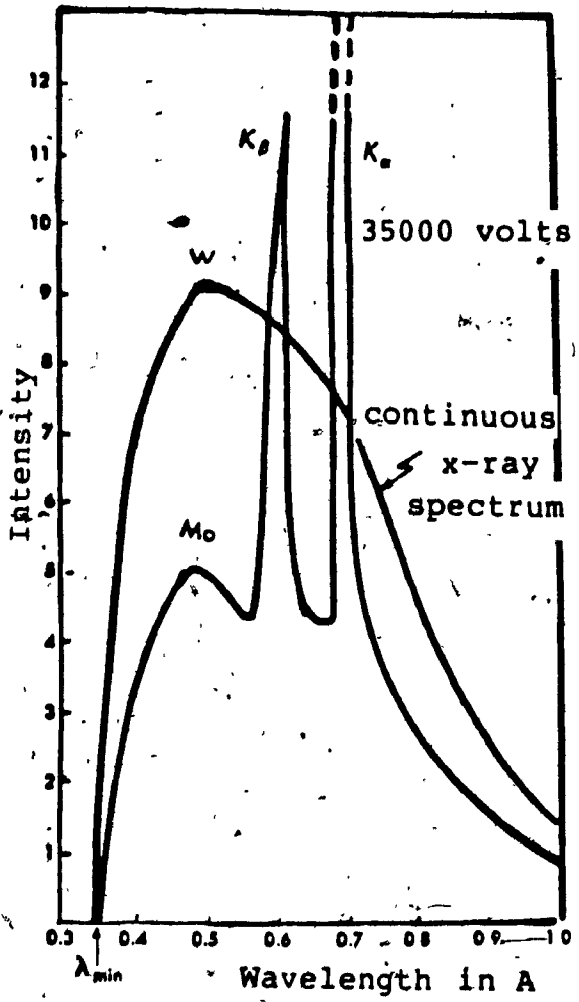

Fig.(2.2)

Fig.(2.1) The continuous x-ray spectrum, results from the radiation emitted by the electrons which are accelerated in the coulomb field of force of the nuclei of the target atoms .

Fig.(2.2) Typical x-ray spectra, obtained by Ulrey (12) from tungsten and molybdenum targets.

2.2.3 Soft and Hard x-rays

The absorption of electromagnetic radiation varies with the energy of the photons and with the type of absorbing medium. Hard and soft x-rays affect the absorbing media in two different ways:

i)A long wavelength or soft x-ray is absorbed appreciably in the material while , ii)A short wavelength or hard x-ray is slightly attenuated through the same thickness of the same material. This clearly shows that for certain materials and for photons of relatively low energy (less than 4Mev) the attenuation coefficient decreases as the energy of the photons increases.

2.3 Gamma-rays

This particular radiation is produced when a nucleus drops from a higher energy state into a lower and more stable one. Actually one cannot make distinction between gamma-ray and x-ray. Today these two terms are used only to distinguish between the sources of the rays

The distinction between γ-ray and other charged particles comes from the mechanism of the absorption of gamma-rays which is indicated by the highly greater penetrating power of this radiation. The fundamental property of gamma rays is the exponential variation of the intensity of radiation as a homogeneous beam of gamma-rays traversesa thin slab of matter.

2.4 Beta rays

Beta rays are particles which are charged negatively. They consist of fast moving electrons which are distinguished from the cathode rays only by velocity (13). During the early experiments it was discovered that beta particles emitted by naturally radioactive nuclides might have velocities up to around .99c. At the same kinetic energy the beta-particles travel much faster than the alpha particles, this is due to the mass of beta-particles which is much less than that of alpha-particles. For instance an α-particle with an energy of 4Mev has a velocity about (1/20c), while a 4Mev electron would have a velocity about .99c.

2.5 Neutrons

The main source of neutrons are nuclear reactions. A neutron does not have a visible track in the cloud chamber. This fact along with extraordinary high penetrating power of the neutrons indicate that its charge must be zero. This means that a neutron has no ionization power. A neutron is heavier than a proton and has a wide application in chemistry, biology and medicine. Principally it loses its energy in collision with nuclei not with electrons. For some applications it is required to have neutrons, in the range of .01ev to a few ev which are called slow neutrons. Fermi (15) and his coworkers obtained slow neutrons by passing them through hydrogenous media (i.e. the neutrons are slowed down without being absorbed).

For biological purposes neutrons are regarded as uncharged particles as gamma or x-rays. Neutrons produce protons by transfering their energy to the hydrogen of tissue.

2.6 Heavy Charged Particles

Heavy charged particles have different applications in nuclear medicine and biology(14). Heavy charged particles produce a more concrete path than electrons with the same velocity, because they have much heavier mass than beta particles and also scattering is almost negligible in comparison with them. The penetration of heavy charged particles depends on its energy, as the energy decreases while passing through the medium. This energy loss gives rise to a maximum specific ionization near the end of the path, which is called Bragg -peak. Heavy charged particles are also very useful in molecular study because of their ability to deposit large amounts of energy in a single macromolecule. The most important application of heavy charged particles is in radiation therapy. It is possible to produce controlled lethal damage in definite locations of interest.

2.6.1 Protons

Protons are hydrogen nuclei having a mass of 1.0075 and a charge of one. It is possible to get energetic protons by artificial means from the cyclotron or a Van der Graaff

generator. Protons are intermediate between alpha particles and beta particles, in their ionization density and penetrating ability.

2.6.2 Deuterons

Deuterons have a mass of two, charge of one and their penetrating properties and ionization density lie between those of protons and beta particles.

Most recent machines have permitted us today to produce particles which carry a charge greater than alpha particle and heavier than that. The particles which are frequently used are carbon, nitrogen, oxygen, and neon.

2.7 Primary and Secondary ionizations

As a consquence of interaction between charged particles with matter, some electrons are ejected. Most of these ejected electrons are of adequate energy to cause some ionization on their own account, which is known as a "secondary ionization". The former one which is produced by interaction of charged particles are called "primary ionization". The ejected electrons which are capable of travelling an appreciable distance and producing additional electrons are called delta rays. These electrons have tracks branching off the main track of the charged particles. Fig.(2.3) enables us to ellucidate the random distribution of ionization produced along the path of ionizing particles.

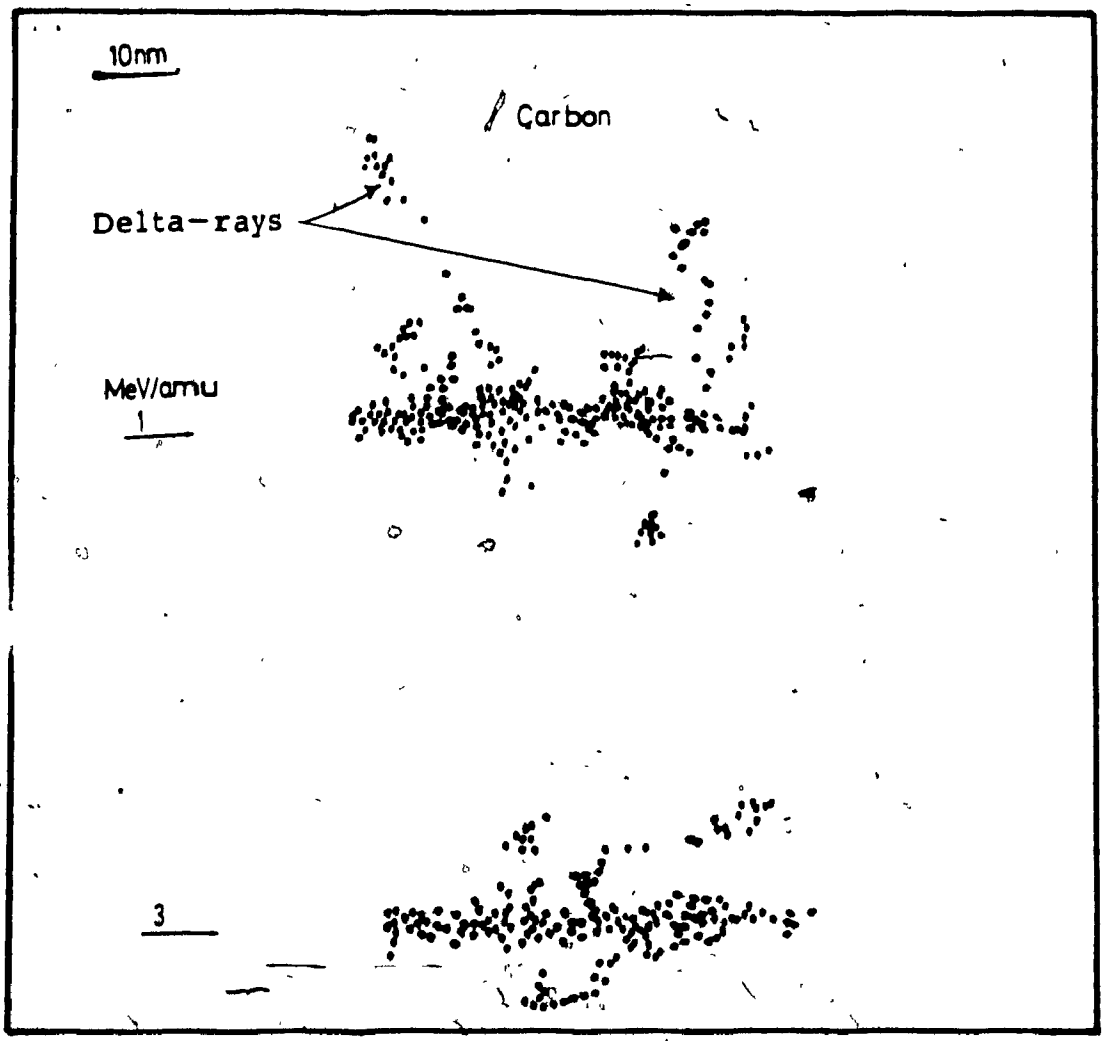

Fig.(2.3) Calculated carbon track segments of 1 and 3 Mev/amu in water vapor with ion track code MOCA-14 (10).

2.7.1 Bragg-Peak

The Bragg curves can be studied experimentally by inserting absorbers of varying thickness into the particle path, and then measuring the ionization density using an ionization chamber. It is of great interest to see that, for alpha-particle near to the end of their range, the Bragg curve obtains its maximum, making about 6000 ionizations per mm of air. At the end of the range the ionization declines sharply to zero.

Ionization in a medium is accompanied by loss of energy the particle each ionization corresponds to an energy loss of about 32ev. Thus the Bragg curve gives not only a measure of the ionization density but also of the energy lost per mm of the path.

2.7.2 Radiation Yields

The effect of absorbed energy in a medium by ionizing radiation is, in the first instance, the production of reactive entities such as ions, excited states, and free radicals. These species can react with themselves or with substrates which may be present in the system and eventually give rise to stable products. For given experimental conditions, the amount of product or the yield resulting from the effect of the radiation will depend on the amount of energy deposited in the system. Yields in radiation studies

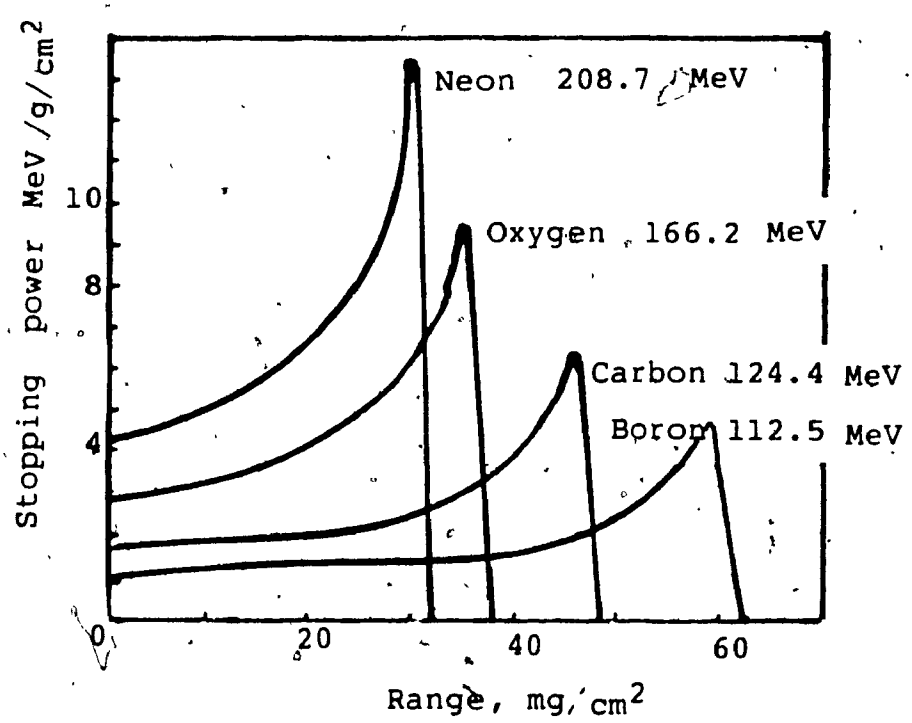

Fig.(2.4) Bragg curves determined for ions of neon, oxygen, carbon and boron and converted to tissue-equivalent material. The energy of each ion is 10.3 MeV/amu.

have been explained in two ways.

2.7.3 Ionic Yield

The radiation study in the past was devoted to the investigation of the ions produced in the gaseous system, and the ions were thought to exert a controlling influence on the chemical changes observed. Yields were, therefore, described as ionic yields, and denoted by (M/N), where M is the number of molecules of the system which have experienced chemical change and N is the number of ions produced in the entire system. The ionic yield is thus the number of molecules changed per ion produced. The energy required to produce an ion pair in gases could be measured; therefore, the ionic yield is an implicit statement of the energy absorbed. In fact most ionic yields have been described as number of molecules changed per 32 eV energy absorbed.

2.7.4 The G-value

In the study of condensed matter, the yield does not have as significant role as in the gaseous system, because the number of ions produced cannot be determined in them. The calculation in this case should be based on the assumption of a value for the energy loss for the formation of an ion pair in condensed matter. In the early studies of the condensed matter, it was thought that the average amount of energy needed to produce an ion pair is the same as for air. Principally, the amount of energy absorbed by a

condensed medium from ionizing radiation can be measured directly. Yield is defined in terms of a G-value , which is the number of molecules changed per 100 eV of energy absorbed, therefore , there is no need to search for the ions produced. If the absorption of 100 eV of energy by molecules of a system resulted in the formation of x molecules of a substance A, these data would be expressed as G(A)=x. In some cases the destruction of a particular compound is considered. If, for instance, y molecules of a substance B were destroyed by the absorption of 100 eV of energy,the result may be expressed G(-B)=y, where the minus sign indicates the destruction of molecules. Ionic yield is expressed mostly as G-value, even for gaseous systems. Essentially, in order to express the results in G-values, the absorbed energy by a system under particular conditions must be known. The determination of the amount of energy absorbed is known as dosimetry and forms the subject of Chapter III.

2.8 Energy Loss by Charged Particles

2.8.1 Introduction

A fast charged particle passing through material makes collisions with atomic electrons provided that the particle is heavier than an electron (proton, deuteron , alpha-particle, etc). The atomic electrons are capable of taking up appreciable amounts of energy from a heavy

incident particle without it being deflected. The loss of energy by the ionizing particle is almost entirely due to collisions. The scattering is restricted to rather small angles, so that, while losing energy, a heavy particle keeps almost a straight path, until it becomes sufficiently close to the end of its range. For incident electrons the energy loss and scattering happens in collisions with atomic electrons. Consquently, the path becomes much less straight. As a matter of fact after a short distance, electrons instead of going in a rectilinear path, tend to diffuse. The emphasis of our discussion is on the physical idea's involved, rather than the exact numerical formulas. We have to acknowledge the fact that even if all basic features are classical or semi-classical in origin, still a quantum mechanical treatment is required in order to get accurate results. The order of magnitude of the quantum effects could easily be inferred from the uncertainty principle. A through investigation on the subject will be followed as the point of departure. The simple problem of energy transfer by a fast heavy particle to a free electron will be studied. Through this investigation the classical Bohr formula for energy loss will be obtained, and the quantum modification will be described in details.

2.8.2 Classical Treatment of the Energy Loss

A fast particle of charge Ze and mass M collides with an electron in an atom. If the particle moves fast in

comparison with the characteristic velocity of the electron in its orbit, the collision can be dealt with as if the electron were free and initially at rest. Another approximation we will make is that the momentum transfer Δp is adequately small such that the incident particle is basically undeflected from its straight path, and the recoiling electron does not move appreciably during the collision. What we require at this stage is the calculation of the momentum impulse caused by the electric field of the incident particle at the position of the electron. The incident particle interacts with the electron of charge e and mass $m<<M$ at an impact parameter b (the distance of closest approach from the electron is called the impact parameter). The angle included by the path of charged particle and by r is labled θ.

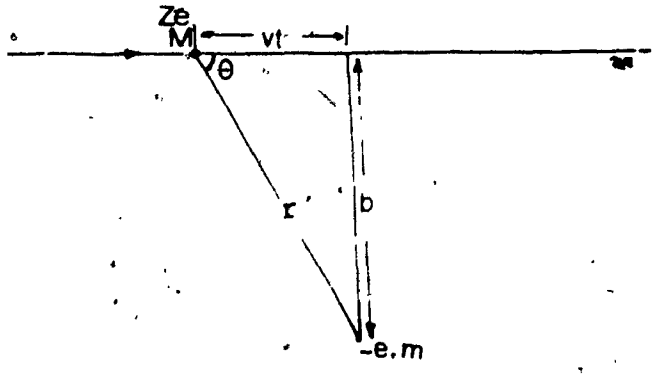

Fig.(2.5) Schematic representation of a collision of a charged particle with an atom.

Using a coordinate system in which x direction coincides with the path of the charged particle and y direction is perpendicular to it. The effects of the force components in

x-direction cancel, that is, the particle is slowed down by such a force component in approaching the scattering center, but is speeded up the same amount by an equal but opposite force component in receding from the center.

Thus, only the component of the Coulomb force acting along the y-direction has a non vanishing time integral.

$$\Delta P_y = \int F_y dy = \int eE_y(t)dt$$

$$E_y(t) = Ze/r^2, \qquad r^2 = b^2 + x^2 \quad \text{or}$$

$$r^2 = b^2 + (Vt)^2, \qquad V \text{ is the particle velocity.}$$

$$E_y(t) = Ze/(b^2 + (Vt)^2)$$

One finds

$$\Delta P_y = -\int_{-\infty}^{\infty} eZe/[b^2 + (Vt)^2]dt = 2\int_0^{\infty} Ze^2/[b^2 + (Vt)^2]dt =$$

$$2Ze^2 \int_0^{\infty} dt/[b^2 + V^2t^2] =$$

$$2Ze^2/V^2 \int_0^{\infty} dt/(b^2/V^2 + t^2)$$

by integrating we have

$$\Delta P_y = 2Ze^2 [(V/b)\arctan(Vt/b)]_0^{\infty}/V^2$$

$$2Ze^2_0[\arctan(vt/b)]^{\infty}/Vb=$$

$$2\,Ze^2\,[1-0]\,/Vb$$

Consequently,

$$\Delta P_y=2Ze^2/Vb \qquad (2.1)$$

The energy transferred to the electron is

$$\Delta E(b)=(\Delta p)^2/2m=2Z^2e^4/mv^2b^2 \qquad (2.2)$$

The energy transfer $\Delta E(b)$ has some interesting characterestics:

i) It varies inversly as the square of the impact parameter, so that the close collision involves very large energy transfer, ii) It depends merely on the charge and velocity of the incident particle not its mass.

Generally speaking, a fast moving particle traversing matter meets electrons at various distances from its path. If there are N atoms per unit volume, we can make the assum-

ption that those electrons are located in a cylindrical shell of length x, and of inner and outer radii b and b+db. The number of electrons located in the cylindrical shell can be calculated as

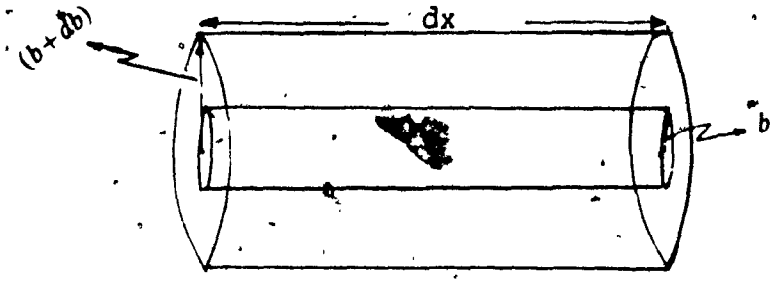

Fig.(2.6) Schematic representation of the interaction of a charged particle with an assembly of atoms.

$$\Delta n=\Delta x[\pi(b+\Delta b)^2-\pi b^2]N=2\pi Nb\Delta b\Delta x$$

and the energy transfer to these electrons will be

$$dE=\int_{b_{min}}^{b_{max}}\Delta E(b)dn=\int_{b_{min}}^{b_{max}}2\pi N\, bdbdx(2z^2e^4/mv^2b^2)=$$

$$(4\pi Ndx/m)(z^2e^4/v^2)\int_{b_{min}}^{b_{max}}db/b$$

or

$$dE = (4\pi Ndx/m)(z^2e^4/v^2)\ln(b_{max}/b_{min})$$

Therefore

$$dE/dx = (4\pi N/m)(z^2e^4/V^2)\ln(b_{max}/b_{min}) \qquad (2.3)$$

To evaluate Eq.(2.3) the limits of the impact parameters bmin and bmax must now be found.

2.8.3 Evaluation of b_{min}

As b tends to zero(b=0) dE tends to infinity which is incorrect. However, the maximum velocity a free electron may obtain in a collision is 2V. This could be seen in the following;

Assume a head on collision, concerning conservative nature of energy and momentum, namely

$$(1/2)MV^2 = (1/2)MV_r^2+(1/2)mv^2$$

$$MV = MV_r+mv$$

where V and V_r are the velocity of charged particle before and after collision and v is the electron velocity. By solving for V_r we will obtain

$$V_r=(Mv-mv)/M=V-(m/M)v$$

substituting

$$MV^2=M[V-(m/M)v]^2+mv^2=M[V^2+(m^2/M^2)v^2-2Vvm/M]+mv^2$$

and using the initial assumption, that is, M>>m in the latter equation, the term m^2/M^2 would be much less than unity; in that case, this term may be neglected and the equation reduces to

$$MV^2=MV^2-2Vvm+mv^2$$

or

$$v = 2V$$

which provides that the actual maximum velocity of a free electron in a collision is 2V. Therefore, the maximum energy transfer is

$$\Delta E_{max}=(1/2)m(2V)^2= 2mV^2 \qquad (2.4)$$

Equating eq.(2.2) to the maximum allowable energy transfer Eq.(2.4).

$$\Delta E(b_{min})=\Delta E_{max}=2mV^2=(2Z^2e^4/mV^2)(1/b_{min}^2)$$

one obtains

$$b_{min} = (Ze^2/mV^2)$$

This can be achieved by another approach very easily. The average velocity of the electron in collision time is given by $\Delta p/2m$ and the time of collision is given by $t = b/V$. Hence, the distance travelled during the collision is of the order of

$$d=(\Delta p/2m)(t)=[(2Ze^2)/(bV/2m)](b/V)=(Ze^2/mV^2)=b_{min}$$

As long as $b>d = b_{min}$, eq.(2.2) is valid

2.8.4 Evaluation of b_{max} .

For large values of impact parameter the electron can not be considered as free. In fact as the collision time is long compared to the vibrational period $(1/\omega)$, the electron will make numerous cycles of motion as the incident particle gradually travels by, and will be influenced adiabatically by the fields without any net transfer of energy.

The dividing point comes at b_{max} where the collision time and the orbital period are comparable. Therefore it seems quite justified to extend the integral to the point where $b/V=1/\omega$ and to neglect contributions from greater b values . Therefore,

$$b_{max} \triangleq V/\omega \qquad)$$

It is expected that for $b>>b_{max}$ the energy transfer descends rapidly to zero Fig.(2.7).

2.8.5 Evaluation of Average Energy Loss

Using Eq.(2.3) and integrating between b_{min} and b_{max} one finds that

$$dE/dx = (4\pi N/m)(Z^2e^4/V^2)\ln(b_{max}/b_{min})$$

or

$$dE/dx = (4\pi N/m)(Z^2e^4/V^2)\ln(mV^3/Ze^2\omega) \qquad (2.5)$$

This approximate expression for the energy loss shows all the basic characteristics of the classical result due to the Bohr. The following is Bohr expression which is discussed in his paper (29).

$$dE/dx = (4\pi N/m)(Z^2e^4V^2)[\ln(1.123mV^3/Ze^2\omega-(V^2/2c^2)] \qquad (2.6)$$

where, $(-V^2/2c^2)$ is a small correction even at high velocities. From the initial assumptions, the condition for the validity of Bohr's formula is

$$Ze^2/mV^2 << V/\omega \text{ or } Ze^2\omega/mV^3 << 1$$

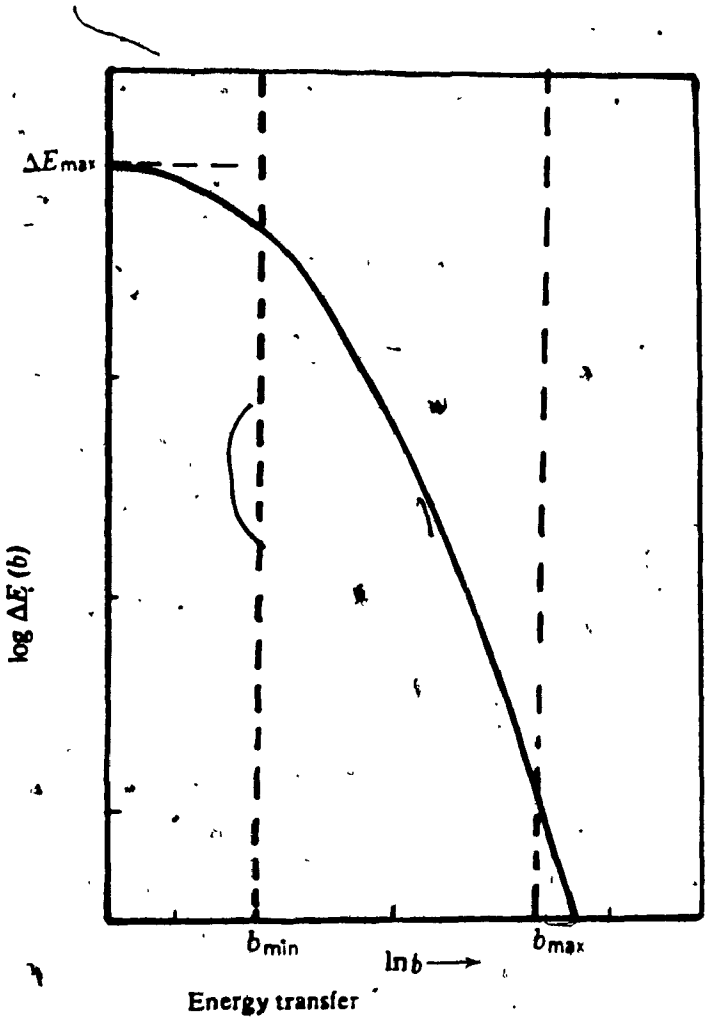

Fig.(2.7) Schematic representation of the region in which Bohr's formula is valid. The condition that is necessary for the validity of this formula is that there be a range of b values in which $b_{min}<b<b_{max}$.

2.8.6 Quantum Treatment of Energy Loss

In this case, it has been assumed that electrons in atoms move like harmonic oscillators. This means that instead of an assembly of atoms we may consider an assembly of harmonic oscillators whose frequencies are equal to the absorption frequencies of the atoms. Let us assume that there are n atoms per unit volume with z electrons per atom. The z electrons can be divided into groups specified by the index i, with fi electrons having the same harmonic binding frequency ω_i. The number f_i is known as the oscillator strength of the ith oscillator. The oscillator strength satisfies the obvious sum rule,

$$\sum_i f_i = z$$

If n atoms are available per unit volume these should be replaced by atoms with nf_i oscillators. Therefore, when a charged particle passes through atom, it affects the electrons of the atom through its electric field. A light wave too will act on an atom by its electric field and it is therefore reasonable to replace the atoms by oscillators and then use the formula for the energy transfer which we had derived, namely

$$dE/dx = (4\pi/m)(Z2e^4/V^2)n \sum_i b_{min} \int^{b_{max}} f_i(db/b) \quad (2.7)$$

where n is the number of atoms per unit volume.

2.8.7 Quantum Evaluation of b_{max}

The function of discrete nature of energy transfer can be explained by the calculation of the classical energy transfer (i.e.Eq.(2.2)). At $b = b_{max}$, the $\Delta E(b)$ would be the smallest energy transfer which is of any significance in the energy loss process. Assuming only one binding frequency ω_o for the purpose of simplicity, it will be found that

$$\Delta E(b_{max}) \simeq 2Z^2 (v_0/V)^4 (h\omega_0) \qquad (2.8)$$

where v_0 is the orbital velocity of an electron, in the ground state of hydrogen. Since $h\omega_0$ is of the order of the ionization potential of the atom. It will be observed that for a fast particle $V >> v_0$, the classical energy transfer is negligible compared to the ionization potential or even to the smallest excitation energy in the atom. But it is well known that the energy should be transferred in certain quanta. A negligible amount of energy like (2.8) can not be absorbed by the atom. This bring us to the conclusion that our classical expression is not effective in this sphere. It should be admitted that this calculation will be correct only if our clsssical formula (2.2) give a quanta energy large enough compared to the excitation energy of the atom. Consquently, the result for b_{max} in classical treatment should be changed.

It is possible to search for an intermediate solution to reconcile the classical and quantum mechanical approach. Applying the statistical model for a classical approach might obtain a desirable result.

Quantum consideration states that the classical result of the transfer of energy in every collision is incorrect. But by considering a large number of collisions, on the average, a small amount of energy is transferred to the each electron. It means, in most collisions no energy is transferred, but in a few collisions an appreceible excitation takes place. For this reason the average value over many collisions is small. In this statistical treatment classical-mechanics and quantum mechanics will end yield the same result. Consquently, it is possible to apply the same expression for b_{max} which come from classical theory, namely,

$$b_{max} = V/\omega_i$$

2.8.8 Quantum Evaluation of b_{min}

In quantum theory it is meaningless to speak about a closer approach between an incident particle and an electron than the de Broglie wavelength of electron or ion.

$$b_{min} = \lambda(\text{de Broglie wavelength}) = h/mV$$

As we have seen, for a non relativistic free particle the wavelength λ of a particle having a momentum $p = mV$ is given by equation $\lambda = h/mV$, where h relates the wave and particle characteristic of the material. The lower limit derived from the quantum mechanical approach has a higher value than that of the classical one. This is due to the fact that any approach closer than the quantum lower limit causes diffraction phenomena. The occurance of this phenomenon will make an effective approach impossible. The lower limit of b could also be obtained by the uncertainty principle, viz.

$$\Delta x \Delta p > h$$

or

$$\Delta x = h/\Delta p = h/m\Delta V$$

thus

$$b_{min} = \Delta x (\text{quantum analog of } b_{min})$$

2.8.9 Quantum Mechanical Energy Loss Formula

Using the limits of b obtained from quantum mechanical approach Eq.(2.7) becomes

$$dE/dx = (4\pi Z^2 e^4/mV^2)[n\sum_i f_i \ln(b_{max}/b_{min})] =$$

$$(4\pi Z^2 e^4/mV^2)[n\sum_i f_i \ln(mV^2/\hbar\omega_i)]$$

or

$$dE/dx = (4\pi NZ^2e^4/mV^2)\ln(mV^2/h\omega_i) \qquad (2.9)$$

This can be compared with the quantum mechanical result of Bethe and Bloch (17) which is given by the following formula,

$$dE/dx = (4\pi NZ^2e^4/mV^2)\ln[(2mV^2/h\omega_i)-(V^2/c^2)] \qquad (2.10)$$

Regardless of the small correction term $(-V^2/c^2)$ and a factor of 2 in the argument of the logarithm, Eq.(2.9) could be considered a good approximation of Bethe's formula. However, Eq.(2.9) is valid if the velocity of the incident particle is much greater than the velocity of an electron. Otherwise, our treatment is no longer valid and the correct treatment for this case has not yet been achieved. If the ion velocity becomes equal to the velocity of the outermost electrons in the slowing down medium, then the charged particles may pull out electrons from the medium, attach them to itself and henceforth reduce its effective charges. While, the charged particle had its charge reduced, its ionizing power and energy loss will also be smaller.

Serious deviation for alpha-particles from the fomula (2.9) begins with somehow higher energy of 200 keV. The corresponding limit for the deuteron is at 100 keV and for the

proton is at 50 keV

2.9 Linear Energy Transfer (LET)

The, linear energy transfer (LET) of charged particles in a medium is the quotient ΔE by Δl where ΔE is the average energy locally imparted to the medium by a charged particle of specified energy in transversing a distance of Δl. The term " locally imparted " may refer either to a maximum distance from the track or to a maximum value of discrete energy loss by the particle.

$$L = \Delta E/\Delta l$$

The linear energy transfer changes from point to point along the path of the particle , reaching a climax at the top of the Bragg curve. We should confirm that the above definition provides the average value of L for the entire path The concepts of energy loss and linear energy transfer are, somehow, different. The linear energy transfer refers to energy locally imparted within a limited volume while energy loss measures energy lost by the ionizing particles, without taking the location of absorption of this energy into consideration. The total LET without considering any energy cut-off is shown as L_∞.

To express the various cut-off levels of delta-ray energy from the main track is labled by the subscript of L. This is the suggestion of ICRP-ICRU(1963)? For instance,

L_{100} represents the delta-rays of energy 100ev or more which are considered as separate tracks.

CHAPTER III

PRINCIPLES OF DOSIMETRY AND MICRODOSIMETRY

3.1 Introduction

The mechanism of the transfer of energy from the radiation field to an absorbing medium was studied during the second chapter. In the following chapter an attempt will be made to investigate the concepts and units employed in specifying the quantity of transferred energy. Any meaningful measurement requires two essential conditions:

i) A clear definition of the concept of the phenomena which are going to be measured.

ii) A clear and comprehensive specification of the unit which is supposed to quantify the measurment.

3.2 Dosimetry Concepts

3.2.1 Dose

In order to specify the dose at a point of interest, in a meaningful way, it is necessary to consider the energy imparted to a small mass of absorbing material, Δm, that is small enough so that further reduction in its size does not change the measurement of the energy imparted per unit mass, but, simultanously is large enough so that a sufficient number of interactions occur within it to enable an accurate estimate of the average energy transfer to be made.

For the purpose of dosimetry, the energy specified is the mean energy locally imparted in the volume element, which is shown as follows,

$$D = \Delta E_d / \Delta m \qquad (3.1)$$

where ΔE_d is the average absorbed energy, Δm is the mass of absorbing material and D is the average energy imparted in the volume element. Until 1975, the two units of dosimetry in common use in radiation biology were the Roentgen(R) and rad (rad). One rad was defined as the absorption of 100 ergs of radiation energy per gram of material.

In May 1975 the General Conference on Weights and Measures adopted new units. The Roentgen is being phased out and there is no special unit for exposure in SI. The SI unit of absorbed dose is the Gray (Gy) and it is defined as 1 joule per kilogram and is one hunderd times larger than the rad (1 Gy= 1 J/Kg=100rad).

3.2.2 Kerma

Kerma is an acronym made of first letters of the phrase " kinetic energy released to matter ". Kerma is defined as kinetic energy released in matter by uncharged particles(photons, neutrons,...) divided by the mass of the scattering element, therefore,

$$K = \Delta E_k / \Delta m \qquad (3.2)$$

In the process of the interacting of uncharged particles with the medium, however, some energy will be transferred from the uncharged particles to charged particles , that is, electrons or protons. Kerma is defined as the sum of all the initial kinetic energy transferred to the charged particles, per unit mass of absorbing medium, thus, ΔE_k, represents the sum of all the released kinetic energy through the matter.

3.2.3 Difference Between Dose and Kerma

The difference between dose and kerma for uncharged particles is illustrated in figure(3.1). Suppose a photon approaches the small mass, Δm, and experiences a photoelectric interaction and transfers the total amount of energy, ΔE_k, to an electron. Of this total amount of energy transferred to the electron only the portion ΔE_d is absorbed in the mass, Δm. The remainder of the energy is absorbed outside this mass. As can be seen, the energy responsible for absorbed dose is ΔE_d, Therefore,

$$D = \Delta E_d / \Delta m \qquad (3.3)$$

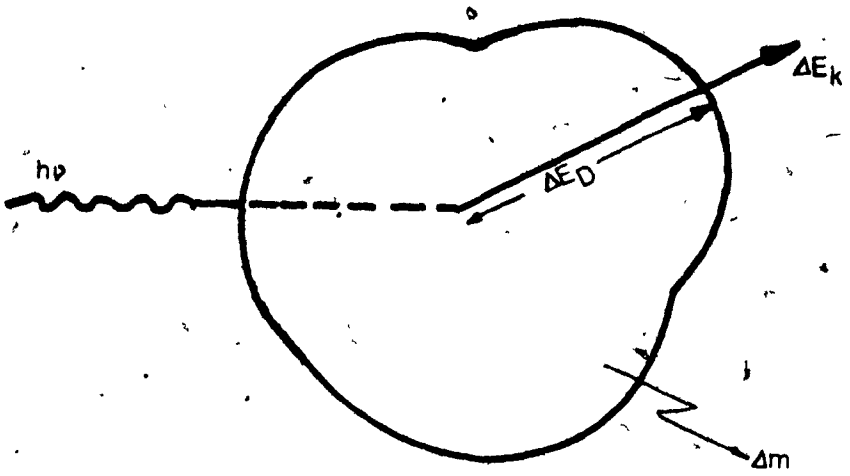

Fig.(3.1) Diagram illustrating the relationship between dose and kerma.

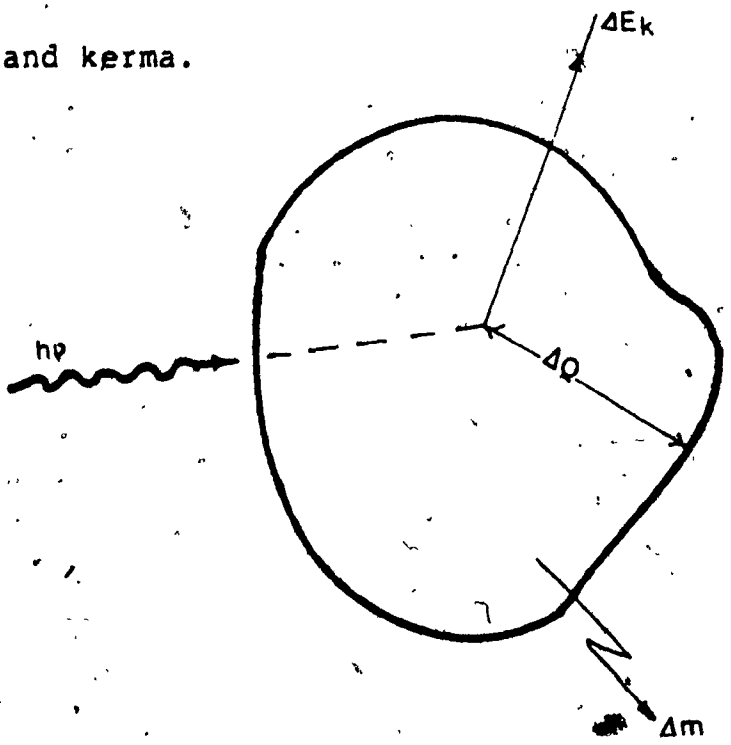

Fig.(3.2) Illustration of the relationship between kerma and exposure.

on the other hand, kerma is responsible for the energy type of ΔE_k. Thus,

$$K = \Delta E_k / \Delta m \qquad (3.4)$$

The unit of kerma is defined as energy per unit mass, for instance, joule per Kg, and kerma rate defined as kerma per unit time.

3.2.4 Exposure

Absorbed dose usually is not measured directly, a conversion factor is needed to find the absorbed dose of various materials. This factor can be achieved by gamma or x-ray exposure. For exposure the type of radiation is limited to uncharged particles and the type of the medium is limited to air. Again exposure as a concept of radiation dosimetry, concerned with the transfer of energy from the radiation field to the medium, and is defined as

$$X = \Delta Q / \Delta m \qquad (3.5)$$

where Δm is volume element of air and ΔQ is the sum of electrical charges on all the ions of one sign that are formed in the air. The special unit of exposure is Roentgen and $1R = 2.58 \times 10^{-4}$ Coulomb/kg of air.

3.2.5 Relationship Between Dose, Kerma, and Exposure

There is a very close relationship between dose, kerma, and exposure in air in experimental situations when electron equilibrium is obtained. Assume a photon beam interacts with the molecules in the air container and produces high speed electrons. As described in section (3.2.2) the total energy transferred to the air is ΔE_k. If the total number of ions formed by the high speed electrons is denoted by N and if the average energy needed to produce one ion pair is w, the kerma is given as follows

$$K = \Delta E_k / \Delta m = (N \cdot w)/\Delta m \qquad (3.6)$$

The exposure can be written as

$$X = \Delta Q / \Delta m = N \cdot e / \Delta m \qquad (3.7)$$

where e is the charge of an ion. From the comparison of Eqs.(3.6) and (3.7) the following consquence can be obtained.

$$X = eK/w$$

Under conditions of electronic equilibrium kerma is equal to absorbed dose thus,

$$X = eD/w \qquad (3.8)$$

The common unit of exposure is called the Roentgen (R).

$$1R = 2.58\times10^{-4} \text{ coul/kg of air}$$

Exposure rate defined as

$$\text{exposure rate} = \Delta X/\Delta t$$

where Δt is the time interval.

3.3 Microdosimetry

3.3.1 Definition

As we have seen absorbed dose is a macroscopic physical quantity like other quantities as specific heat or density. The usefulness of this quantity is that it determines the energy transferred in the volume of interest. Microdosimetry is a refinement in dose based concepts(20). Due to the different responces of biological systems to equal absorbed doses of different radiations, the study of local energy densities and their stochastic nature of distribution become important in this field. The application of microdosimetry to radiobiology consists in

efforts to derive information on the mechanism of the biological action of radiation from a knowledge of such distributions.

3.3.2 Specific Energy

The local energy density which is called specific energy is defined as an energy deposited by ionizing radiation localized in a region with mass m divided by the mass. The symbol for specific energy is z and it is measured in units of Gray,

$$z = E/m \tag{3.9}$$

where E is the energy deposited in a volume element m.

The average of specific energy is defined as absorbed dose D. In other words if the number of events is very large, z equals to D. In microdosimetry, also another quantity which is as equally important as specific energy is defined below.

3.3.3 Lineal Energy Density

It seems a reasonable requirement to compare energy deposition in a volume of different sizes by a characteristic dimension of the volume such as mean diameter, d, namely

$$y = E/d \qquad (3.10)$$

where y is lineal energy density which is defined only for single energy deposition events, and d is the mean diameter of the volume of interest which is refered usually as a mean chord length

It is convenient to express the energy in this case in keV, consquently, lineal energy density will be defined in the units of keV/micrometer

3.3.4 Relationship Between Quantities

In the previous sections it was shown that the energy is a common factor between the quantities, namely

$$E = z.m = d.y = \bar{l}.y$$

or

$$y/z = \bar{l}/m \qquad (3.11)$$

where m is mass of volume element and $\bar{l}$ is the mean chord length of the same volume. As we know for convex bodies $\bar{l}$ is four times the volume divided by the surface (22),

therefore,

$$z/y = (4v/s)/m = (4v/s)/(p.v) = 4/p.s \qquad (3.12)$$

Applying appropriate units in Eq.(3.12) we have

$$z(rad) = 67(y/p.s) \qquad (3.13)$$

CHAPTER IV

CLASSICAL TARGET THEORY

4.1 Introduction

Target theory implies that " one or more ionzations anywhere within a particular structure of biological system (for instance,an enzyme) are sufficient to cause lethal damage ". The sensitive part which is struck by ionizing radiation is called a "target". This target is of volume v and represents the size of a sensitive element of irradiated material. Generally speaking, the region within which ionization has to be produced to obtain the lethal damage or mutation is defined as the target. The passage of an ionizing particle through the target producing ionization (i.e.lethal damage) could be called a "hit". The type of action which is our interest is caused by a single-hit. The hit can be defined as follows

i) The ionizing radiation when passing through the material loses its energy in discrete quanta.

ii) Each hit interacts independently and obeys a poisson distribution.

iii) The inactivation occurs when the sensitive part receives one or more hits.

4.2 Dose Response Relationship

When biological systems are irradiated, different responses are produced most of which increase with absorbed

dose, but are not proportional to it (4).

4.2.1 Single Event Response

It is convenient to say that the total number of hits is simply proportional to the dose of a given radiation in one hit action (21). The number of targets hit is proportional to the dose, and a straight line is obtained by plotting the survival fraction versus dose, Fig.(4.1a). Its properties can be characterized as follows:

i) The survival curve is exponential.

ii) The effect of a given dose is constant, and does not depend on the rate at which the dose is delivered.

iii) For producing equal effects, required dose differs for different ionizing radiations.

Speaking empirically, if a dose dD acts on the target the surviving fraction of material will be decreased by the amount of dn, namely

$$-dn/dD \propto n$$

or

$$dn/dD=-kn \qquad (4.1)$$

therefore

$$\ln(n/n_0) = -kD \qquad (4.2)$$

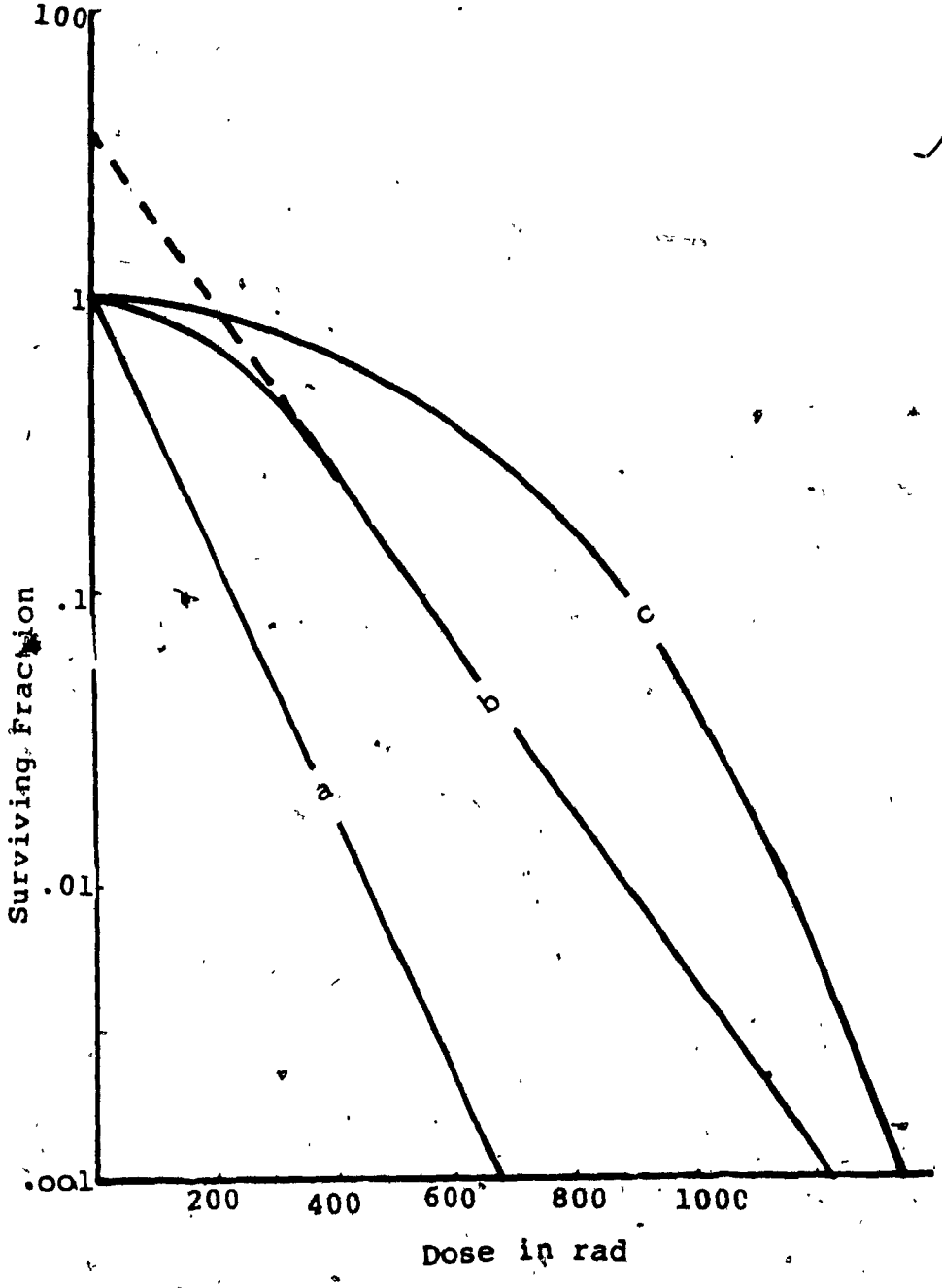

Fig.(4.1) Survival curves: (a) Single event survival curve. (b) Multi- event survival curve. (c) Continuously increasing rate of survival curve.

which can be demonstrated in exponential form

$$n/n_0 = \exp(-kD) \qquad (4.3)$$

Where n is the survival number, n_0 is the initial quantity of material, and n/n_0 is the ratio of activity which remains after a dose D. The following discussion seems necessary for equation (4.1). First of all, this is a linear equation with the slope of k, (4b), which differs for different molecules. Therefore, k could be considered as a basis for estimating target size. Thus by specifying the dose, and measuring the corresponding survival fraction (n/n_o), k could be determined. Essentially when each sensitive element receives one hit the following expression will hold.

$$kD^{37}=1 \qquad (4.4)$$

which gives rise to $\ln(n/n_0)=e(-1)=.37$.

Consquently, it could be indicated that 37% survival fraction of the survival curve represents the "MEAN LETHAL DAMAGE".

$1/D^{37}$ is called the radiosensitivity which will be discussed extensively later on.

4.2.2 Multi-Event Response

The exponential curves, we have seen in single-event responses are observed for high LET, while multi-event responses are induced by low LET radiation. In this case the survival fraction after producing a shoulder is represented by an exponential curve Fig.(4.1b). The region within which the survival fraction increases is called the shoulder of the curve. This is due to the accumulation of lethal damage in biological systems which is sufficient to produce the observed effect (21b, 22). The form of this curve is given by an expression which is obtained by the poisson distribution as follows.

In low LET when the number of ionizing particles experienced by a cell is large, it is reasonable to make the assumption that each cell receives the same average dose. Therefore, we can say , if the average number of lethal lesions per cell is denoted by A_1, the survival fraction would correspond to the probability of receiving no lethal lesion, namely

$$S = \exp(-A_1) \qquad (4.5)$$

The above argument is concerned with the simplest case of the problem.

In general the average dose is misleading if applied directly to individual cells, therefore the survival fraction must be related to the average number of lethal damages A_1 by a more general relationship (27). Assume the mean number of lethal damages produced in sensitive sites(i.e. multitarget) of a cell is A_1. The probability of experiencing no lethal damage by the sensitive site in a cell is $\exp(-A_1)$ and the probability of one or more lethal damages

$$p1 = 1-\exp(-A_1) \qquad (4.6)$$

When n particles passes through a cell the mean number of lethal damage is nA_1. In this case the probability of no lethal damage is $\exp(-nA_1)$ and the probability of one or more lethal damage is

$$Pn = 1-\exp(-nA_1) \qquad (4.7)$$

Eq.(4.6) can be written as

$$1-p_1 = \exp(-A_1)$$

then

$$\exp(-nA_1) = (1-p_1)^n$$

Substituting in eq.(4.7) we have

$$P_n = 1-(1-p_1)^n \qquad (4.8)$$

For a population of cells exposed to a mean fluence of N particles through sensitive sites of mean projected area s, the probability of n particles through a given area s, is the nth term of a poisson distribution, such as follows.

$$N^n/n!\exp(-N) \qquad (4.9)$$

Therefore, the probability of one or more lethal damage in a given cell will be

$$P_N=0\sum^{\infty} P_n(N^n/n!)\exp(-N) \qquad (4.10)$$

Replacing P_n from Eq.(4.8) will give

$$P_N = 0\sum^{\infty}[1-(1-p_1)^n](N^n/n!)\exp(-N) =$$

$$P_N = 0\sum^{\infty}(N^n/n!)\exp(-N) - 0\sum^{\infty}[(1-p_1)^n](N^n/n!)\exp(-N)$$

$$0\sum^{\infty}(N^n/n!)\exp(-N) = (1+N+N^2/2!+N^3/3!+\ldots)\exp(-N) =$$

$$[\exp(N)]\exp(-N) = 1$$

$$0\sum^{\infty}(N^n/n!)[(1-p_1)^n]\exp(-N) =$$

$$0\sum^{\infty}\{[N(1-p_1)^n/n!\}\exp(-N) =$$

$$\{1+N(1-p_1)+[N(1-p_1)]^2/2!+[N(1-p_1)]^3/3!+\ldots\}\exp(-N) =$$

$$\exp[N(1-p_1)]\exp(-N) = \exp(-Np_1)$$

Therefore

$$P_N = 1 - \exp(-Np_1) \qquad (4.11)$$

The surviving fraction of cells would be

$$S = n/n_0 = 1-[1-\exp(-Npl)] = \exp(-Np_1)$$

or

$$S = n/n_0 = \exp\{-N[1-\exp(-A_1)]\} \qquad (4.12)$$

For $A_1 << 1$ this leads to the generally used Eq.(4.5).

4.2.3 Other Response Shapes

Another type of response has been observed in which the dose effect keeps on increasing throughout the whole range of Fig.(4.1c). This type of curve is difficult to analyse, unless some assumptions are invoked concerning the rate of increase. As an example, assume that the rate of increase is constant. In this case the first order of its derivative relative to the dose gives a straight line, from which

$$S = \exp[-(k_1D+k_2D)D]$$

Generally, for this type of curve no obvious simplifications are possible. Some attempts have been made by Sinclair(21), and Kellerer(22), and some interesting approaches are suggested, but this topic will not be discussed in this paper.

4.3 Relative Biological Effectiveness (RBE)

4.3.1 Definition

According to the agreement of ICRP-ICRU(1963) the relative biological effectiveness of one ionizing radiation compared with another (usually with different LET) is defined as the inverse ratio of their doses which give the same type and degree of biological effect provided that all other factors except the dose and LET stay the same. This will include both the radiation parameters and medium parameters.

4.3.2 Relative Biological Effectiveness for Single Event Response

The type of dose response curves is particularly important in deriving the relative biological effectiveness of two radiations. For a one-hit process, the RBE is simply defined as the ratio of dose of reference radiation(r) to the test radiation(t)

$$S = \exp(-k_t D_t) = \exp(-k_r D_r)$$

or

$$k_t D_t = k_r D_r$$

Therefore

$$RBE = k_t/k_r = D_r/D_t \qquad (4.13)$$

If our reference is gamma-ray, then

$$RBE = D_\gamma/D_t \qquad (4.14)$$

Let us consider a hypothetical case in which alpha-particle radiation produces ten times as much biological effect per rad as does gamma-ray. The RBE for that particular biological effect would be 10.

No mystique or magic determines the RBE for one type of radiation versus another, and there is no adequate theory that tells us what the RBE should be, or must be, for a particular type of radiation.

4.4 Calculation of Molecular Weight from Survival Curve

If the reason for inactivation of a molecule is the occurance of one ionization in a volume v, therefore, we can say the probability of ionization in one cluster in a sensitive volume v is vI, and the probability of n_o cluster is given by exp(-vI) which is equal to the value of the surviving fraction.

namely

$$S = n/n_o = \exp(-vI) \qquad (4.15)$$

where v is the volume of the target molecule and I is the number of ion clusters per unit volume.

To make use of ionizing radiation as a means of measuring molecular weight in biology the following empirical equation has been used by many authors. If the total energy dissipated per unit distance is dE/dx and the energy required to produc one ion pair is w, the ratio of energy loss and w will introduce the number of ionizations produced by a single ionizing radiation per unit distance, that is

(dE/dx)(1/w)=Average number of ions produced per unit distance

The total number of ionization per unit volume produced per unit distance would be the product of (dE/dx)(1/w) and the number of ionizing particles per square centimeter. This gives the following result.

$$I = (dE/dx)(1/w)(f) \qquad (4.16)$$

where f is the number of particles per square centimeter. As we have seen, when each sensitive element receives one hit, the following expression will hold

$$vI = 1 \tag{4.17}$$

Substituting for I in expression (4.17), this will give us the volume of molecules

$$v = w/[f(dE/dx)] \tag{4.18}$$

therefore, the mass of a molecule would be presented as below

$$m = vd = wd/[(dE/dx)f] \tag{4.19}$$

where d is the density of a given material. Recall that molecular weight (Mw) or mass of one mole of molecules is given by the following well known formula,

$$Mw = (NA)m \tag{4.20}$$

where NA is Avogadro's number and m is the mass of a

molecule.

$$Mw = (w)^2(d)(NA)/(dE/dx)f \qquad (4.21)$$

The molecular weights of different molecules were calculated by the above formula and are tabulated in Table I. The data used in these calculations were taken from Pollard et al (5), Brustad (6b), and Dertinger and Jung (23). These results will be discussed later in section 4.6.

4.5 Cross-Section

The case of inactivation by heavy charged particles where the events are localized along tracks but at intervals of the order of magnitude of the molecular dimensions, has been attacked from two different approaches. Lea (4b) considers the volumes associated with the primary ionizations to overlap, therefore putting more than one event in the same space and wasting some of them. Pollard et al (5a) on the other hand proceed in a manner applied in poisson distribution and calculate the probability, p, of at least one ionzation occuring in the thickness of the molecule of interest.

At this point we shall outline the first order empirical calculations. If dD ionizing radiations per unit area are fired through an enzyme sample, the chance of a particle passing through a molecule of cross- sectional area A is AdD. Then if we let p be the probability of one or more ionizations

Table I

CALCULATED MOLECULAR WEIGHT BY RADIATION METHOD

Material	Calculated (Mw) Daltons	Reportyed Size Daltons	Energy of incident particle
Trypsin	32000	15000-24000	Deuteron (4MeV)
	34000		Electron (2MeV)
Pepsin	49000	36000-39000	Deuteron (4MeV)
Chymotrypsin	30000	23000	Deuteron (4MeV)
Catalase	52000	250000	Deuteron (4MeV)
Invertase in yeast	112000	120000	Deuteron (4MeV)
Succinic dehydrogenase	82000	80000	Electron (2MeV)
Ribonuclase	13000	13000	Proton (2MeV)

in the molecule if an ionizing particle passes through it, we find for the chance of inactivation

$$-dn/dD = pAn$$

where the probability p for the occurence of an interaction between an ionizing radiation and one atom is illustrated by a cross-section, namely

$$\sigma = pA$$

Therefore

$$-dn/dD = \sigma n$$

or

$$n/n_o = \exp(-\sigma D) \qquad (4.22)$$

where n/n_o is the surviving fraction remaining after a total dose of D, σ is the inactivation cross-section which represents the chance of inactivation per incident radiation.

4.5.1 The relationship between inactivation cross-section (σ) and geometrical cross-section (A).

A purely empirical approach allows us to apply a

statistical analysis to the correlation of the inactivation cross-section to the observed geometrical cross-section. If the average number of primary ionizations per centimeter is i and the average thickness of the molecule of interest t, the average number of ionizations per molecular thickness is (it). According to the poisson distribution the probability of no ionization is exp(-it), and therefore, the probability of one or more ionization becomes [1-exp(-it)]. Thus, by substituting for p in Eq.(4.22) leads to the following result.

$$\sigma = A[1-\exp(-it)] \qquad (4.23)$$

The quantity i can be calculated from the experimentally determined rate of energy loss assuming an average of 110eV expended per primary ionization. It can be seen that as i increases, the inactivation cross-section converges to a geometrical cross-section. For fast electron irradiation (it) is very small and expansion of the exponential term in Eq.(4.23) will lead us to

$$\exp(-it) = 1+(-it)+(1/2)(-it)^2+\ldots$$

Hence

$$\sigma = A[1-(1-it)] = Ait = Ati = vi \qquad (4.24)$$

or

$$\sigma = vi \qquad (4.25)$$

where v is the volume of the molecule in question. If both sides of equation (4.25) are multiplied by D, the dose in particles per centimeter square, we obtain

$$\sigma D = viD = vI$$

demonstrating the equivalence of Eqs.(4.15) and (4.23) for this case. From Eq.(4.25) we can see that the slope of the graph of variation of s against i at the origin equals the volume.

4.5.2 Calculation of Molecular Weight from Cross-section

Charged particle inactivation data can yield information about the shape of the irradiated molecules, for instance, the results of irradiating pepsin and trypsin with deuterons are shown in Fig.(4.3). Detailed calculations based on the theory outlined above indicate agreement with those of the previous section. Taking the extrapolated cross-section from Fig.(4.3) (i.e. 1.3×10^{-13} cm^2), the radius of an assumed spherical trypsin molecule is 21A. Utilizing 21A for radius and assuming the density of dried protein 1.3

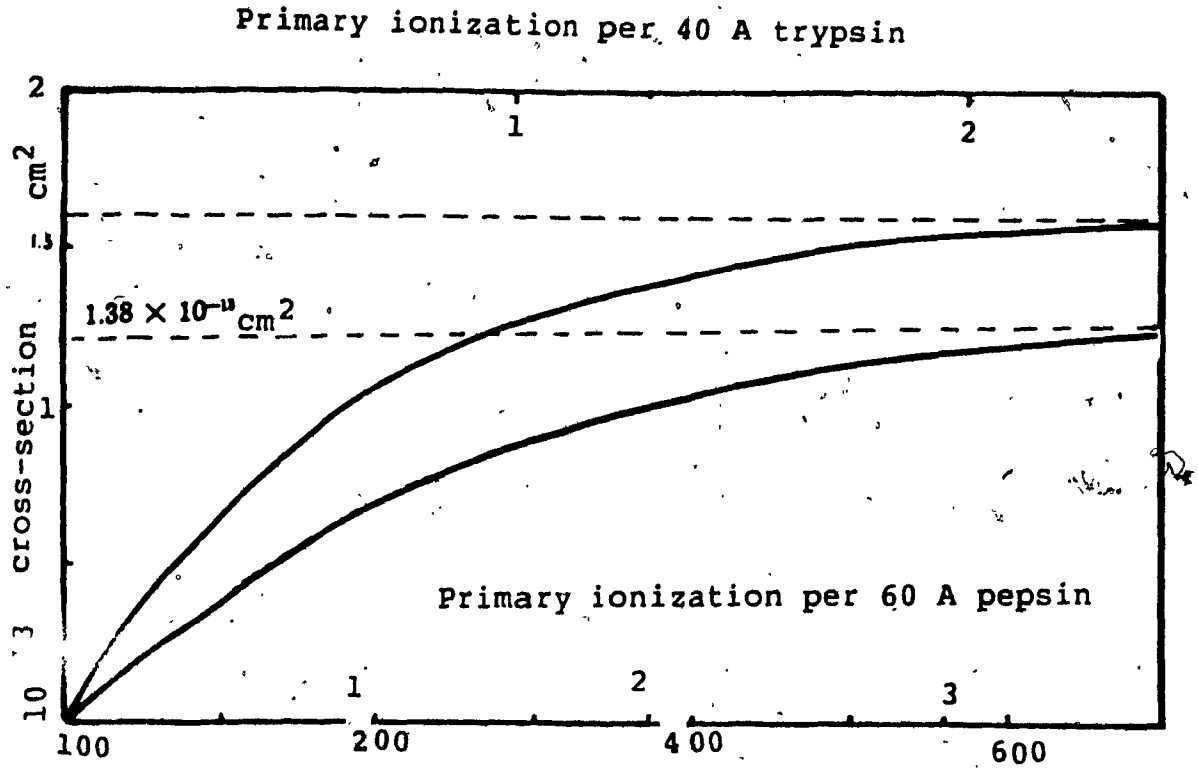

Fig.(4.2) Deuteron bombardment of trypsin and pepsin. The experimental values of deuteron bombardment of trypsin and pepsin plotted against the ionization density. The curve is the function [1-exp(-x)] where x is the theoretical number of primary ionizations per 40 A of trypsin and 60 A of pepsin.

g/cm^3, the molecular weight of trypsin can be calculated as follows

Volume of molecule of trypsin = $4\pi r^3/3 = 4\pi(21\times10^{-8}/3 = 3.88\times10^{-2})$ cm3

Therefore the mass of one mole (M) = $v \cdot N \cdot d = 3.88\times6.02\times1.3\times10^{30} = 30600$ g.

The accepted molecular weight of trypsin is in the vicinity of 24000, and calculated size with another method as in the previous section is (32000- 34000). The molecular weight as determined in the same way is 39000. This is rather higher than the accepted value of 36000 (5b).

4.6 Discussion on Classical Target Theory

The list of radiation "molecular weights " given in Table I shows clearly that this technique gives information which approximately is parallel to information obtained by completly different methods. An investigator who knew only the relative sensitive volumes obtained from this type of radiation data would form a picture of proteins which would agree approximately with that available today. In reality one must concede that all of this work involves the use of hypotheses, which might be more or less exact, in deducing the structure of the protein molecule from the various types of measurements. In practice, the available information is

strictly limited by the complexity of this problem. It appears that there has been a theoretically unjustifiable preoccupation with the details of the molecular size and structure. A hypothesis of a single primary ionization as a reason for inactivation along the ion's path seems an inadequate hypothesis for this purpose, because it neglects the knowledge of the transverse distribution of secondary ionizations along the ion's path. Nevertheless, as the understanding develops, the method will not become worse; rather it may be expected to improve itself more and more. In Chapter V the new approach on radiation study will be discussed.

CHAPTER V

TRACK STRUCTURE

5.1 Track Structure of Katz Approach

5.1.1 Introduction

The inactivation of biological systems by charged particles was discussed extensively in Chapter IV with the concept of deposited energy in a sensitive volume. All attempts with different approaches based on the model that to correlate the inactivation of a system to the molecular size either with dose- response curves or with cross-section and LET relation failed. It seems that in spite of the progressive steps have so far been taken, the problem has not been solved in detail. In another words, as long as the LET does not include knowledge of the transverse distribution of energy along the ion's path, inactivation cross-section cannot be derived from LET, because it neglects the saturation or overkill near the ion's path.

We will see that the cross-section does not directly depend on molecular size and the molecule will be inactivated through the influence of gamma-ray D^{37} rather than a heavy charged particle itself (9). In another words, the cross-section is related to the cross-sectional area of coaxial cylinders whose axis is the track core within which the deposited energy is equal or greater than the gamma-ray

D_{37} . Also in this new approach, there would not be any arbitrary separation between "core" and "cloud" interaction; that is, the separation of secondary electrons into a core in which the dose is perfectly lethal, and a cloud of low intensity will not be considered further.

The significant parameter is taken to be the deposited energy delivered to the medium by all electrons ejected from the ion's path (delta-rays).

We consider here only single event processes in dry materials in which one or more ionizations within the sensitive site is responsible for inactivation. For this purpose the biological systems are thought to consist of sensitive sites embedded in a passive matrix in which a single molecule loses its function if one of its many bonds at a sensitive site is broken.

5.1.2 Evidence for Inadequacy of LET

A decisive point occurred with the work of Brustad (6a), in which Trypsin, Lysozyme and DNase were irradiated by proton, carbon and neon ions. The radiosensitivity of these is given in Fig.(5.1).

As can be seen from the graph the radiosensitivity decreases with increasing LET, and a radiosensitivity of a neon with 187.5 keV/micrometer is half of the radiosensitivity of a 1.5 keV/micrometer proton per bombarding particle. Therefore, we can write,

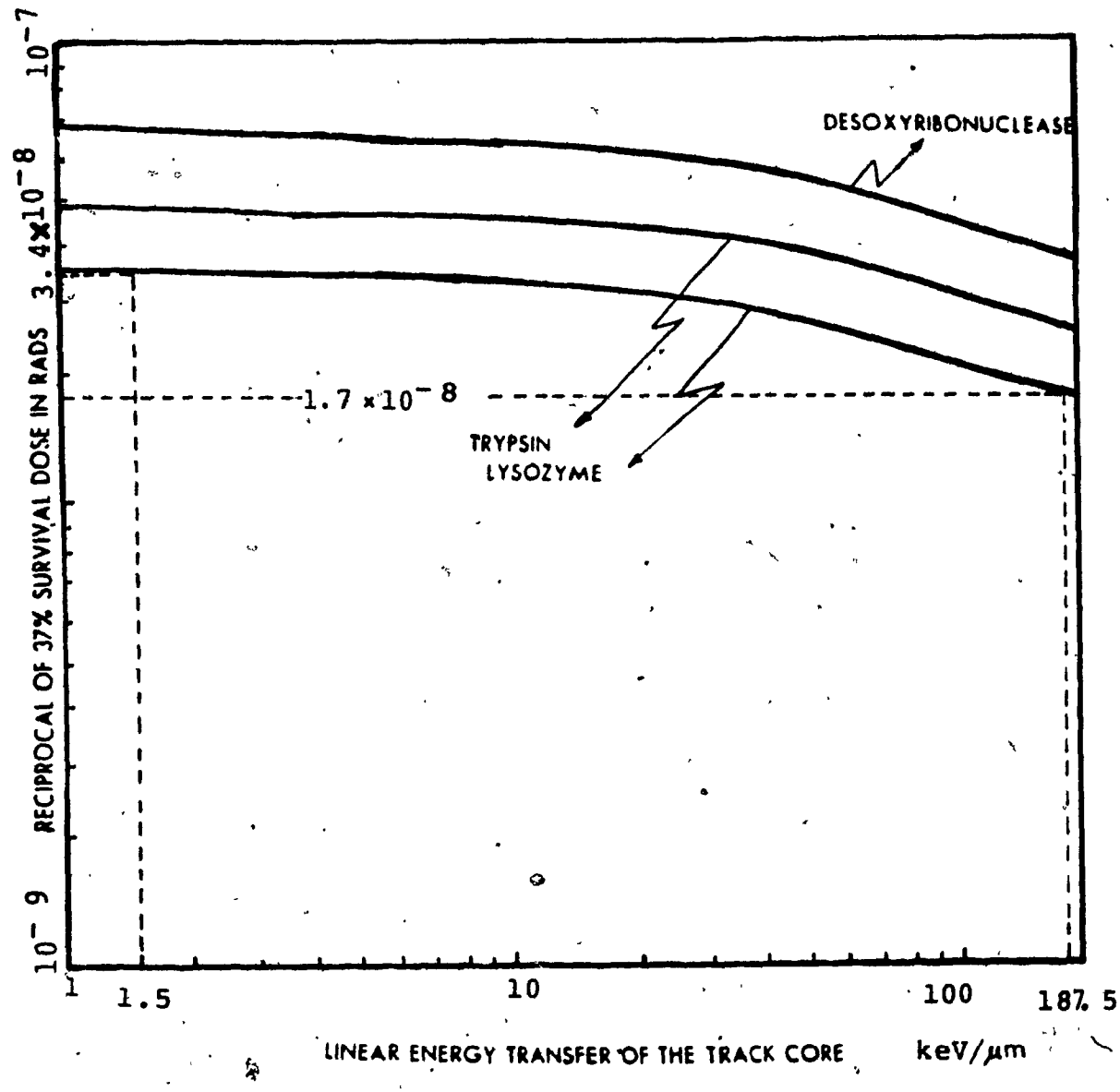

Fig. (5.1) The radiosensitivity of lysozyme, trypsin, and DNase plotted as a function of the LET of the track core of the radiations used. The radiosensitivity is expressed as the reciprocal of the 37% survival dose. (Track core LET ≈ .6 total particle LET).

(Radiosensitivity of proton)/(radiosensitivity of neon) per particle=

$(3.4 \times 10^{-8})/(1.7 \times 10^{-8})=2$

The inactivation cross-section, which is called the effectiveness per ionizing radiation and is [labled ( )] is increasing with increasing LET. According to the Fig.(5.2) the inactivation cross-section of neon (300keV/micrometer) is 50 times larger than the inactivation cross-section of a 3 keV/micrometer proton per bombarding particle (see Eq.(4.23)). Therefore,

(σ of neon)/(σ of proton) per particle=

$(6.6 \times 10^{-13})/(1.3 \times 10^{-14})=50$

In biological terms the effectiveness of a proton is 50 times more than the neon per bombarding particle.

The inactivation cross-section of highest LET is 15 times larger than the geometrical cross-section which is calculated by physico-chemical method (6a). Therefore,

$\sigma/\sigma_o=(6.6 \times 10^{-13})/(4.4 \times 10^{-14})=15$

In the case of neon for example 93% of inactivation cross-section is due to the delta-rays which are produced transversal to the ion's path. So we write:

Delta-rays inactivation cross-section%=

$(6.6 \times 10^{-13} - 4.4 \times 10^{-14})/(6.6 \times 10^{-13}) \times 100 = 93\%$

Consquently, in order to stand with target theory a drastic track structure study should be invoked.

5.1.3 Radial Dose Concept

In a system uniformly irradiated with gamma-rays, mean lethal dose of Y-rays, ${}_{\gamma}D^{37}$, is the dose at which there is one ionization (or hit) per sensitive element. If the system is irradiated with gamma-rays to dose ${}_{\gamma}D$, then from poisson distribution (Appendix A), the probability that any one element experiences one or more ionizations is

$$P=[1-\exp(-{}_{\gamma}D/{}_{\gamma}D^{37})]$$

We may assume a cylindrical shell of length h and radius x with the thickness dx whose axis is the ion's path. If N_o is the number of targets, the number of hits inside the shell is given by

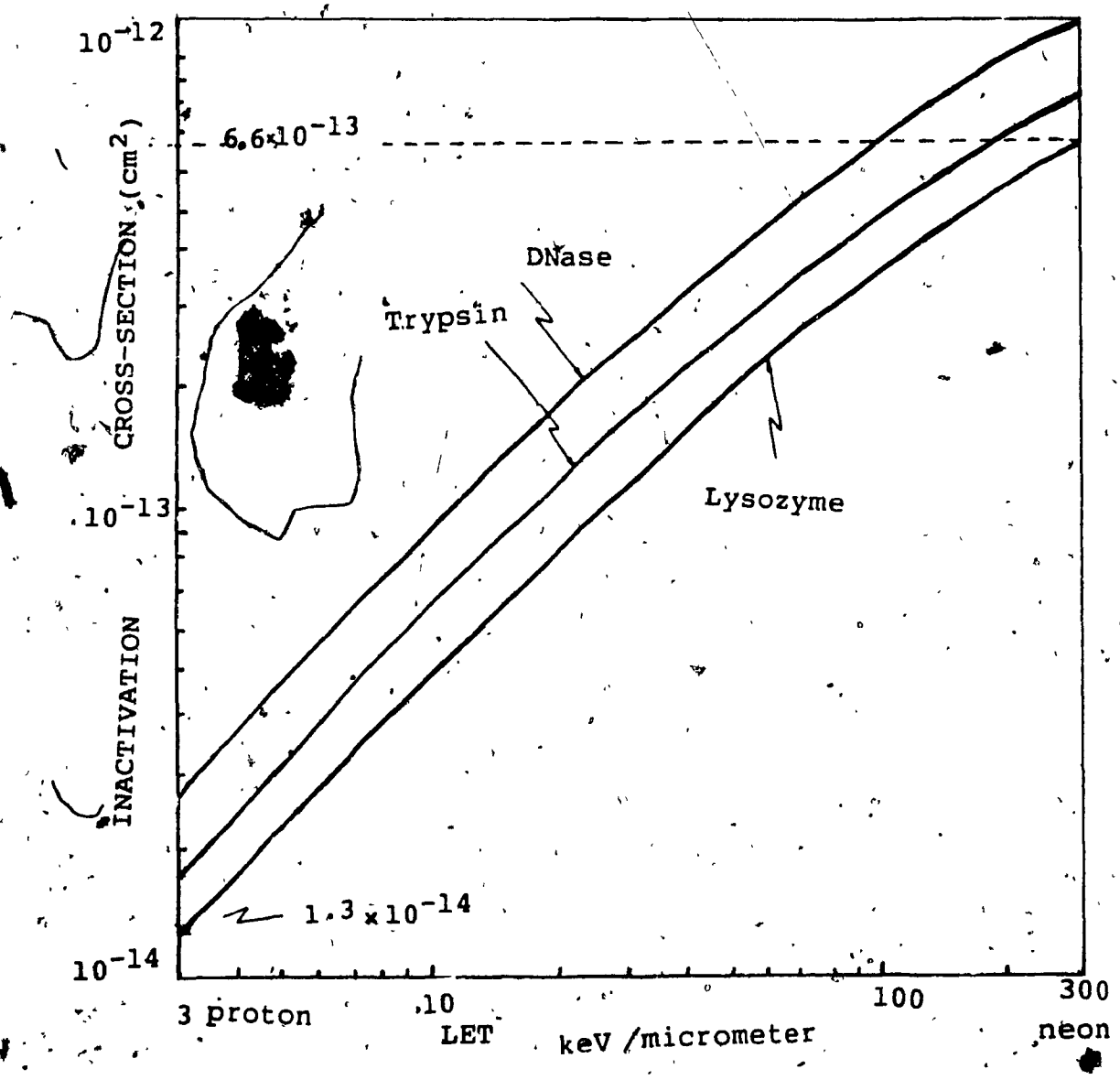

Fig.(5.2) Inactivation cross-section of three enzymes as a function of the LET of track core. Inactivation cross-section is determined from the exponential survival curve, $n/n_o=\exp(-\sigma D)$.

$$\xi = {}_0\int^{\infty} \pi N_o h x [1-\exp(-D_\delta(x)/{}_\gamma D^{37})]dx \qquad (5.1)$$

where $D_\delta(x)$ is the energy per unit volume delivered by delta-rays, which is distributed uniformly over the entire shell. Eq.(5.1) gives the number of inactivations by a single ion passing through a medium. The cross-section is defined as the quotient of the total number of targets hit and the number of targets per unit area, or

$$\sigma = (\xi/N_o h) = 2\pi {}_0\int^{\infty} x [1-\exp(-D_\delta(x)/{}_\gamma D^{37})]dx \qquad (5.2)$$

The above calculation is valid for a point target.

In order to evaluate the equation (5.2) it is required to derive an expression for D_δ as a function of the radial distance, x, from the ion's path. This can be obtained by using a simplified form of delta-ray distribution formula namely

$$dn = [2\pi N e^4 z^{*2} dw]/[mc^2 \beta^2 w^2] = C[z^{*2} dw]/[\beta^2 w^2] \qquad (5.3)$$

where dn is the number of delta-rays per unit path length having energies between w and w+dw, produced by an ion of

effective charge z* (25) moving with speed βc. We approximate biological material by water for which $N=3.35\times10^{23}$ electrons per cm^3. To take into account the mass m and charge e of an electron and the number density electrons in the materials (N) the coefficient , C, will take the value of 8.5×10^{3} keV/micrometer.

The Barkas charge pick up expression z* is represented as follows

$$z^*e=ze[1-\exp(-125\beta z^{-2/3})] \qquad (5.4)$$

By integrating of Eq.(5.3) the total number of delta-rays arising from the passing ion will be obtained

$$n=8.5\times10^{-3}[z^{*2}/\beta^2]\int dw/w^2=8.5\times^{-3}[z^{*2}/\beta^2](1/w_x - 1/w_{max}) \qquad (5.5)$$

where w_x is the energy of a delta-ray just sufficient to penetrate the cylinder if it is ejected normally and $w_{max}=2mv^2\gamma^2$ is the maximum delta ray energy determined by kinematics considerations in head on collision. To complete the calculation we need the range energy relation of equation $x=kw^{\alpha}$ in which by adjusting the value of k its power (α) approaches to one , that is, x=kw or $w=k^{-1}x$. By

replacing this in Eq.(5.5) we have

$$n=8.5\times10^{-3}[k^{-1}z^{*2}/\beta^2](1/x-1/X) \qquad (5.6)$$

where

$$X=k^{-1}w_{max} \qquad (5.7)$$

To find the total energy deposited per unit volume in the cylindrical shell of radius x carried by delta-rays, we multiply the total number of penetrating delta-rays by the energy deposited by each electron and divide by the volume of the shell, $(2\pi x dx)$, to obtain

$$D_\delta(x,\beta,z^*)=8.5\times10^{-3}[k^{-1}z^{*2}dw/\beta^2(2\pi x dx)](1/x-1/X)$$

or

$$D_\delta(x,\beta,z^*)=8.5\times10^{-3}[z^{*2}/2\pi x\beta^2](1/x-1/X) \qquad (5.8)$$

By introducing Eq.(5.8) in Eq.(5.2) we have the explicit form of inactivation cross-section σ

$$\sigma=2\pi_0\int^X x\{1-\exp((-8.5^{-3}z^{*2}/2\pi x\beta^2{}_\gamma D^{37})(1/x-1/X)\}dx \quad (5.9)$$

we have plotted the D/z^{*2} versus radial distance x for water in Fig.(5.3). The dose drops off very rapidly with distance, x. The curve for $\beta=.01$ in Fig.(5.3) is to be taken as arising from upper limits on σ. The Eq.(5.9) integrated numerically and the results plotted versus ${}_\gamma D^{37}/z^{*2}$ with various β. For a wide range of ${}_\gamma D^{37}/z^{*2}$ the inactivation cross-section could be determined from the Fig.(5.4). In this calculation, we assumed that the electrons are ejected perpendicular to the ion's path. As can be seen this assumption is causes a serious error at $\beta=.01$. For ${}_\gamma D^{37}/z^{*2}<3\times10^7$ the inactivation cross-section stays constant provided that $\beta=.01$, because in the limit of very sensitive materials inactivation cross-section is calculated by

$$\sigma=\pi X^2$$

where X is the maximum range of a delta ray. The theoretical results shown in equation (5.9) and Fig.(5.4) have been recalculated to investigate the variation of inactivation cross-section versus LET (see Fig.(5.5)), where ${}_\gamma D^{37}$ takes respectively the values of 10^2, 10^3, 10^4, 10^5, 10^6 Gy and z the valuesof 1, 2, 6, 10, 18, with the velocity range of that in the limit of fast ions (small LET) and

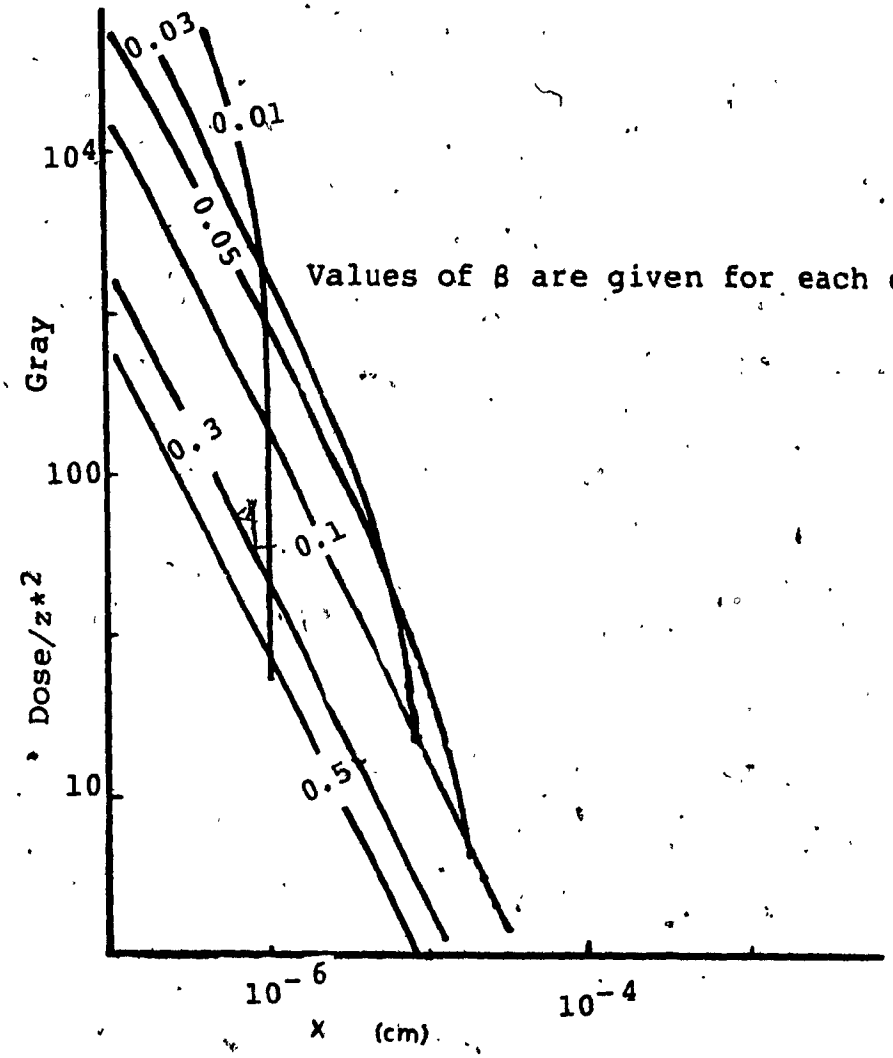

Fig.(5.3) Dose as a function of radial distance from the ion's path for an ion with different velocities. The dose drops off very rapidly with distance.

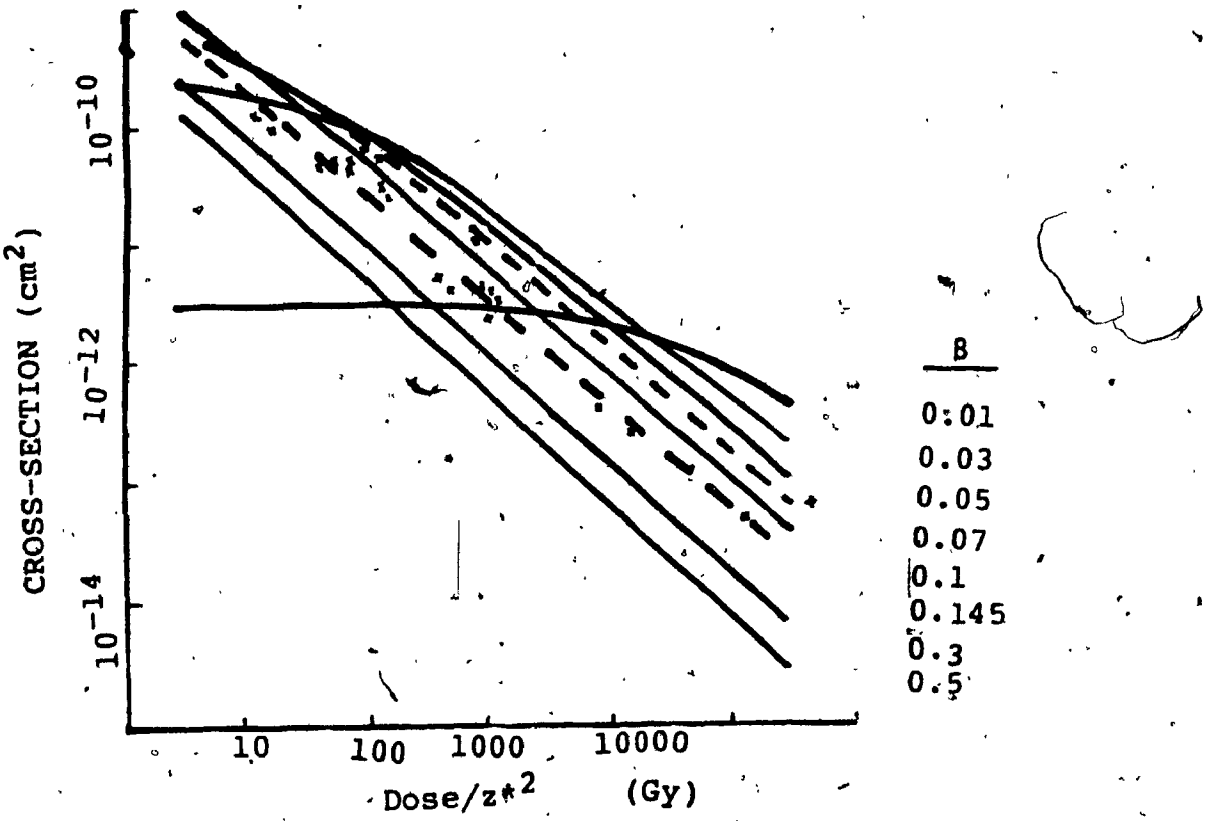

Fig.(5.4) Illustrating the relationship between inactivation cross-section and γ-ray mean lethal dose. Experimental data for β =.07 and 0.145 for two viruses and two enzymes (T1 phage, φx-174 phage, Trypsin and β-galactosidase) are shown superimposed on the theoretical curves (dashed lines). Solid lines represent the theoretical relationship between cross-section and γD^{37} for a variety of bombardments.

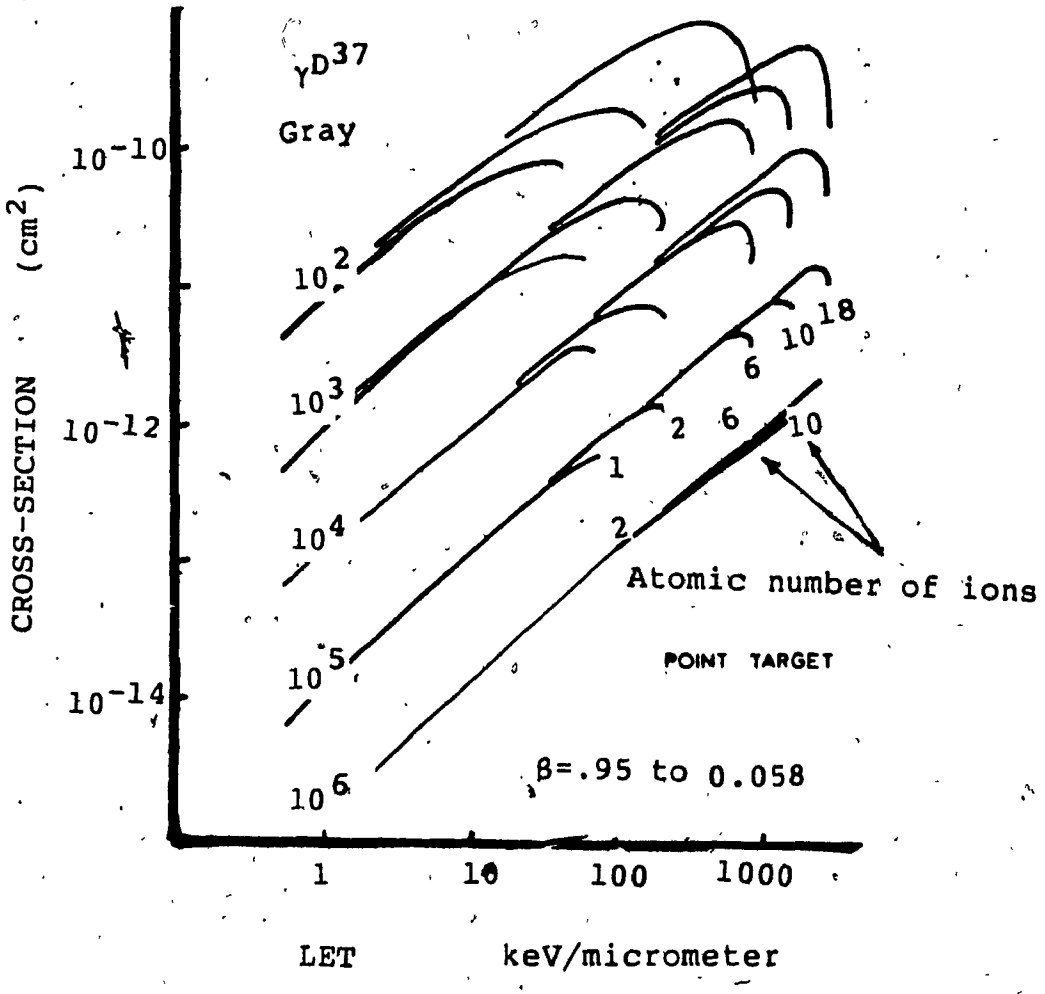

Fig.(5.5) Inactivation cross-section versus LET for dry enzymes and viruses obtained by Katz. The set of curves for different γD^{37} branch according to the atomic number of the ionizing particles.

insensitive materials (large $_{\gamma}D37$) the inactivation cross-section is proportional to LET while at the opposite limits the saturation or overkill appears. In spite of many approximations involved in this model, it scored a good agreement with experimental measurments dealing with collision of heavy ions with enzymes and viruses. These reliable results confirm that the inactivation cross-section are only indirectly related to the actual physical cross-section of the target, for these materials.

The function of this model could be interpreted as the correlation of inactivation cross-section by heavy ions to gamma-ray doses through the spatial distribution of ionization energy arising from the ion's path.

From the comparison of the present work with previous results it appears that heavy ion inactivation cross-sections are related to delta-ray inactivation doses through the spatial distribution of ionization energy arising from the ion's passage. This approach suggests that, the molecular size affects the cross-section, σ, for heavy ion bombardment only very indirectly, through its influence on the, $_{D}37$, for gamma-ray inactivation. It also predicts that, in the limit of low LET and in the case of insensitive materials (large $_{\gamma}D^{37}$) the cross-section is simply proportional to the LET (i.e. in agreement with Brustad's result), while at the opposite limits the relation is complicated by saturation or overkill near the ion's path [See Figs. (5.2) and (5.5)].

5.2 Track Structure of Paretzke Approach

5.2.1 Generating of Random Variables

The term " random variable " is used in order to confirm that one does not know what specific value this variable will take on a given case. The only information we have about a random variable are its range of values and their respective probabilities. We will explore now a general way of generating random variables. Assume that integer numbers from 0 to 9 are written in separate identical papers. Putting them together in a box and picking at "random" one paper at a time and putting it back in the same box, one will obtain a certain distribution of numbers, which could be represented as a table. In that table these numbers have been tabulated in arbitrary digits. Such a table is called a random number table, and could be stored in the memory of a computer. It is clear that for generating a more efficient table of random numbers we need a more sophisticated device than a box. For instance, an example of such a device could be noise signals in electron tubes. For this type of genetrating to be useful one would undoubtedly need a specialized computer designed to apply the numbers to the Mont Carlo method. However, beside several other shortcomings, economically it would not be correct to reduce a multipurpose computer for such a special case with only sparse use to obtain random numbers. For the above reasons it is most expedient to use the so-called ", psuedo-random numbers ".

The latter can be defined as "numbers calculated by means of a prescribed formula and simulating the values of a random variable". As it is clear such a formula must be an ingenious one. Typically, the numbers obtained by the systematics established by the formula satisfy a set of tests insuring a uniform distribution of the psuedo-random numbers on the segment (0,1). Henceforth, these numbers simulate the values of a random variable R. A general expression for obtaining a continuous random variable x can be found by the following

$$R={}_0\int^{x} f(x')dx' \qquad (5.10)$$

where x can represent, depending on the context, the distance to the next event, energy of secondary electron, scattering angle, time interval between two consecutive requests, and so forth.

5.2.2 Calculation of Mean Free Path Length

If the path length of an ionizing radiation, x, is a random variable, distributed in the interval $(0,\infty)$ with the probability density

$$f(x)=a[\exp(-ax)] \qquad (5.11)$$

By applying in Eq.(5.10) we would have

$$R={}_0\int^{x} a[\exp(-ax`)]dx`=1-\exp(-ax)$$

Then

$$\exp(-ax)=1-R$$

Or

$$x=(-1/a)\ln(1-R) \qquad (5.12)$$

The distribution of variable (1-R) is identical with that of R, therefore it could be written as

$$x=(-1/a)\ln R \qquad (5.13)$$

where a is the radiation flow density, R is a uniformly distributed random number within (0,1) and x is the length of the path from one collision to another which could be generated by the aid of random number R.

5.2.3 Monte Carlo Method

The Monte Carlo method can be used simulate on a

computer a large number of track structures of ionizing radiation (photons, neutrons, charged particles) event by event. For this purpose the following steps are required:

1) Adequate cross-sections for relevant process in the material of interest should be invoked. Also it would be appropriate to precalculate for all relevant processes the ratios of their cross-section. For instance the interaction of neutrons with matter is characterized by two constants which are called the capture cross-section and the scattering cross-section. The probability of each type of interaction is given by the ratios of any of them to the total cross-section ;

2) Mean free path lengths between subsquent collisions for primary and secondary particles should be divided and stored by the aid of random numbers (R).

3) Each collision point of ionizing radiation should be described by a fixed Cartesian coordinate frame and a local spherical coordinate frame in each point of collision with moving origins. Also the new direction cosine will be defined after each collision by the aid of Euler angle transfomation in the local frame.

In the field of radiation studies, the track structure is probably the area where the Monte Carlo method is used more frequently than anywhere else.

5.3 Outline of Method Used to Obtain Deposition of Energy in a Given Target Size by Monte Carlo Method

Since this work is based on information obtained from the data book (11), a brief explanation of the method used to obtain the data is required.

For analysis of the data it is assumed that cylindrical volumes of various sizes are oriented at random near tracks of protons and alpha-particles. In this model the tracks of heavy charged particles are enclosed by a virtual cylinder of a radious large enough to contain the tracks of ionizing particles [see Fig.(5.6)]. The virtual cylinder was crossed by chords arranged at random and these form the axes of target cylinders. These target cylinders were subdivided into shorter cylinders of given length. The frequency of deposition of a given amount of energy in each cylinder was normalized to that which would be expected from unit dose. The random distribution of the chords near the central axis of the virtual cylinder was examined for uniformity. Further details of the calculation may be found in the data book (11), where protons with energies between .3 MeV and 4 MeV and alpha-particles with energies between 1.2 MeV and 20 MeV. were treated. Table II is an example of data provided by (11).

From the vantage of the present work we see that,

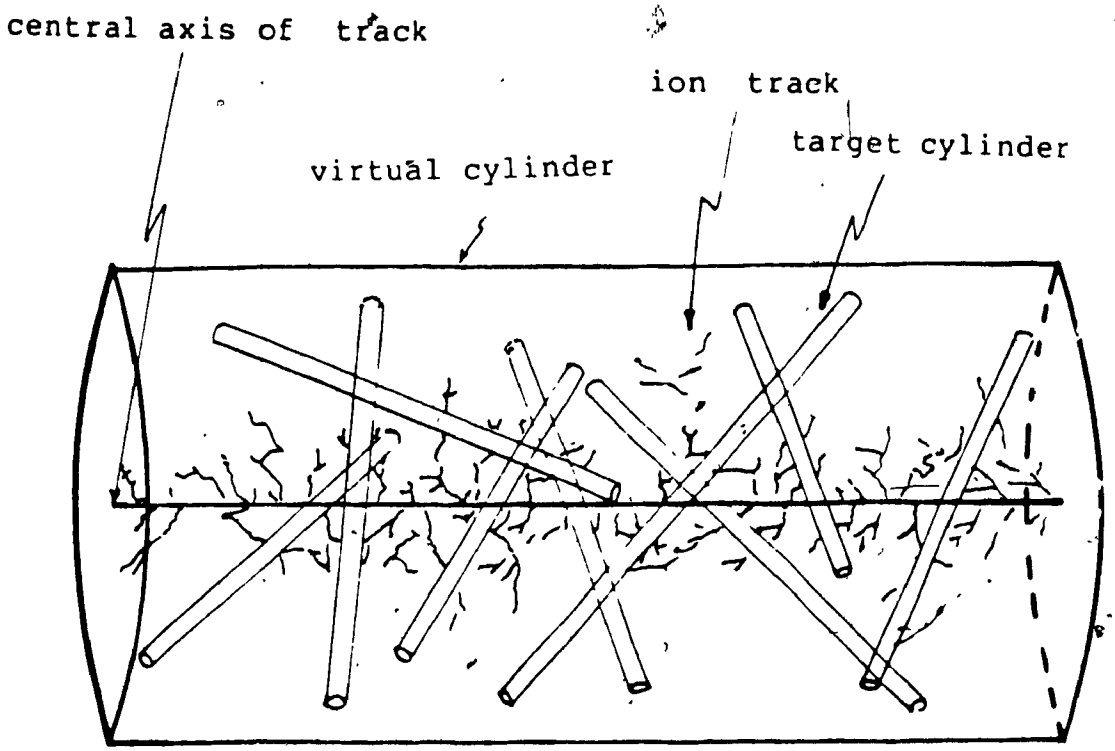

Fig.(5.6) This structure explains how the track segments were enclosed by a virtual cylinder, and shows generated target cylinders traversing the virtual cylinder. Segments of ion tracks were generated using the code (MOCA-14) of Charlton et al (11).

TableII

FREQUENCY OF ENERGY DEPOSITIONS GREATER THAN E PER RAD

Particle; Alpha Energy=.3 MeV/amu

Average stopping power=230.1 keV/micrometer

Total track length scored; 2500.0 nm

Number of infinitely long cylinders hit; 5348

Diameter of target; 3 nm

Target cylinder length(nm)

E (eV)	15	30	60	120	240
0	8.290E-09	1.183E-08	1.794E-08	2.903E 08	5.078E-08
20	5.420E-09	8.222E-09	1.316E-08	2.244E 08	4.088E 08
40	3.798E-09	6.222E-09	1.046E-08	1.843E 08	3.453E-08
60	2.905E 09	5.099E-09	8.854E-09	1.600E 08	3.021E 08
80	2.343E-09	4.269E-09	7.726E-09	1.430E 08	2.730E-08
100	1.927E-09	3.604E-09	6.734E-09	1.277E 08	2.466E 08
120	1.654E-09	3.148E-09	5.976E-09	1.166E 08	2.268E 08
140	1.457E-09	2.825E-09	5.403E 09	1.058E 08	2.088E 08
160	1.294E-09	2.543E-09	4.915E-09	9.826E 09	1.941E 08
180	1.169E-09	2.372E 09	4.601E 09	9.234E 09	1.830E 08
200	1.055E-09	2.177E-09	4.307E-09	8.675E 09	1.723E 08
220	9.374E-10	2.005E-09	4.005E-09	8.201E 09	1.640E 08
240	8.343E-10	1.874E-09	3.796E-09	7.764E 09	1.564E 08
260	7.353E 10	1.764E-09	3.576E-09	7.401E 09	1.496E 08
280	6.424E 10	1.615E-09	3.386E-09	7.054E 09	1.414E 08
300	5.608E-10	1.488E-09	3.168E 09	6.611E 09	1.343E 08
320	4.720E-10	1.383E-09	2.984E 09	6.279E 09	1.273E 08
340	4.082E-10	1.262E-09	2.815E 09	5.976E 09	1.227E 08
360	3.404E-10	1.147E-09	2.653E 09	5.609E 09	1.156E 08
380	2.842E-10	1.045E-09	2.513E 09	5.246E 09	1.095E 08
400	2.276E-10	9.440E-10	2.358E-09	4.944E 09	1.043E 08
420	1.847E-10	8.511E 10	2.157E 09	4.666E 09	9.830E 09
440	1.516E-10	7.624E-10	1.980E-09	4.372E 09	9.144E 09
460	1.255E-10	6.726E-10	1.849E-09	4.107E 09	8.728E 09
480	1.000E-10	5.919E-10	1.659E 09	3.833E 09	8.075E-09
500	8.369E-11	5.174E-10	1.549E-09	3.580E 09	7.560E 09
520	7.042E-11	4.480E-10	1.392E-09	3.254E 09	6.915E 09
540	5.460E-11	3.899E-10	1.263E 09	2.939E 09	6.401E 09
560	4.337E-11	3.388E-10	1.112E-09	2.658E-09	5.870E-09
580	3.521E-11	2.868E-10	9.859E 10	2.380E 09	5.225E 09
600	2.960E-11	2.449E-10	9.001E-10	2.143E-09	4.784E 09
620	2.347E 11	2.082E 10	7.654E 10	1.919E 09	4.278E 09
640	1.480E-11	1.776E-10	7.083E 10	1.755E-09	3.903E 09
660	1.123E 11	1.490E 10	6.225E 10	1.600E 09	3.601E 09
680	9.695E 12	1.327E-10	5.634E 10	1.470E-09	3.233E 09
700	6.634E-12	1.092E 10	5.144E 10	1.314E 09	2.931E 09
720	4.593E-12	8.267E-11	4.715E-10	1.204E 09	2.670E 09
740	3.572E-12	6.736E 11	4.327E-10	1.094E 09	2.417E 09
760	2.551E-12	5.307E-11	3.776E 10	1.012E 09	2.213E 09
Z (rad)	1.227E+08	8.600E+07	5.672E+07	3.505E+07	2.004E+07
Hits	16246	11548	8180	5111	3220

The product of diameter (D) of the target with its length (L) represents target volume and is denoted by (D x L) nm2.

the body of the table is the frequency of hits of energy greater than a given amount in single cylinders when orientated in random in a field of ions delivering one rad of dose. The frequency averaged mean hit size $\bar{z}$ is at the base of the column . This is calculated from the data of the Table II . $(1/\bar{z})$ is the probability of a hit of any size and should equal the frequency of a hit greater than zero. Finally the number of hits on which the statistics are delivered are given at the bottom of each column.

5.4 Comparison with Katz

The sensitivity of biological systems to different ions can be described in terms of inactivation cross-section. Many papers present a model for calculation of inactivation cross-section. The measured cross-section is related to several parameters, such as: size; structure; linear energy transfer and so on. In this thesis the inactivation cross-section was calculated from the equation given in the paper by Goodhead et al (27).

$$\sigma\ (\ cm^2\ ) = (16L/D^{37}) \times 10^{-8} \qquad (5.14)$$

where L is, linear energy transfer, given in keV/micrometer and D^{37} is expressed in rad.

If P(E) is the probability of depositing more than

energy E in a target per rad, and E is selected as the minimum energy required to inactivate the target, then at the mean dose to inactivate a target, D^{37}, [see Eq.(4.3)],

$$D^{37} \times P(E)=1$$

This is equivalent to saying that on average one energy deposition event depositing energy greater than E occurs in the target at the D^{37} dose. Equation (5.14) now becomes

$$\sigma \ (\ cm^2 \ )=(16L)[P(E)]10^{-8} \qquad (5.15)$$

(Values of P(E) constitute the body of the Table II.)

This equation can now be used to compare inactivation cross-sections with those of Katz [see Fig.(5.5)]. The basis of the curves shown in this figure is the gamma-ray dose to inactivate 63% of the targets. In order to compare equation (5.15) with these results it is necessary to choose a target and a threshold energy corresponding to this $_{\gamma}D^{37}$.

To compare with the least sensitive target used by Katz, ($_{\gamma}D^{37}=10^8$ rad) a small target was used and the data in reference (11) were examined at lowest LET (4 MeV protons, LET=10.2 keV/micrometer), for small targets. Two sizes and thresholds (2x2 nm^2 16 eV; and 3x3 nm^2 and 50 eV) gave cross-sections comparable with those of Katz at 10^8 rad when the probabilities were put into equation (5.15). These two sizes and thresholds were then used for other LETs for

protons and alpha-particles and the results shown in Fig. (5.7) are compared with the cross-section from Katz for $_{\gamma}D^{37}$ $=10^8$ rad.

The results show that the two choices of target size and threshold straddle the curve of Katz with similar slopes, over a wide range of LETs.

For larger targets (a smaller value of $_{\gamma}D^{37}$ in Katz's data) a similar proceedure was followed for $_{\gamma}D^{37}=10^6$ rad. Here a size of 20x20 nm^2 with an inactivation threshold 190 eV was used. Again the data are in very good agreement.

One feature of the Katz data, namely the rapid decrease in cross-section at the larger LET for ions (found for larger target sizes) , is smoother with the new calculations, perhaps as a result of using a finite rather than a point target.

5.5 Comparison with Experimental Data

It is useful to also compare this method of calculation with experimental work. Fluke and Forro (28) measured the inactivation cross-section for dry T1-bacteriophage as a function of LET for protons and alpha-particles. Figure (5.9) shows their data .

To compare with the calculation, the volume of the sensitive region of the bacteriophage was estimated to be (30x30) nm^2, using approximately this volume (25x50) nm^2, a

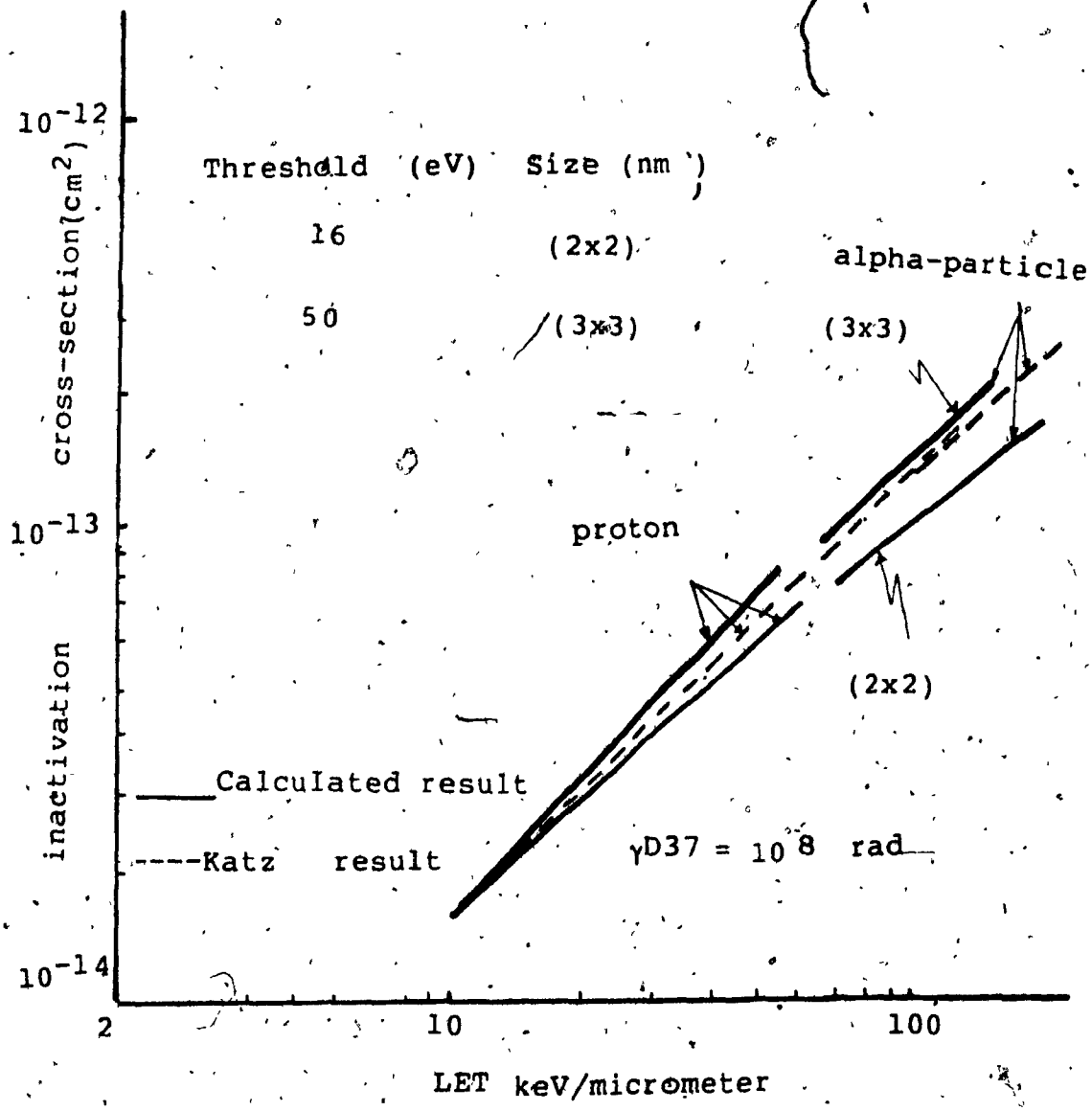

Fig.(5.7) Inactivation cross-section curves for target sizes (2x2) and (3x3) nm2 compared with Katz's data.

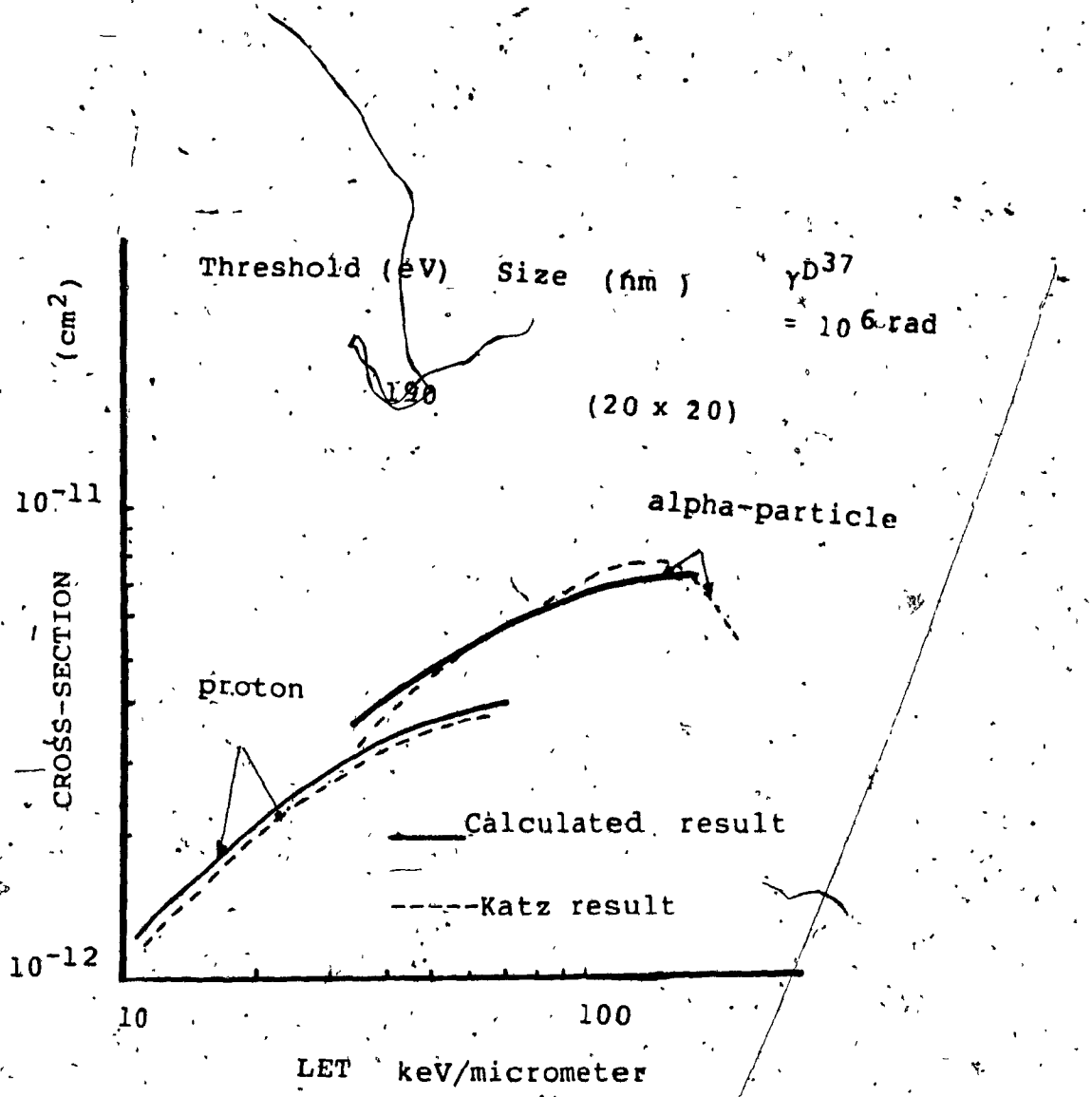

Fig.(5.8) The variation of inactivation cross-section with LET for target size of (20x20) nm^2 compared with Katz's data.

threshold of 250 eV, equation (5.15) was used to calculate the cross-section over the range of LETs used in the experiment. The results are shown in Fig.(5.9) as a solid line. The agreement with experiment is particularly good.

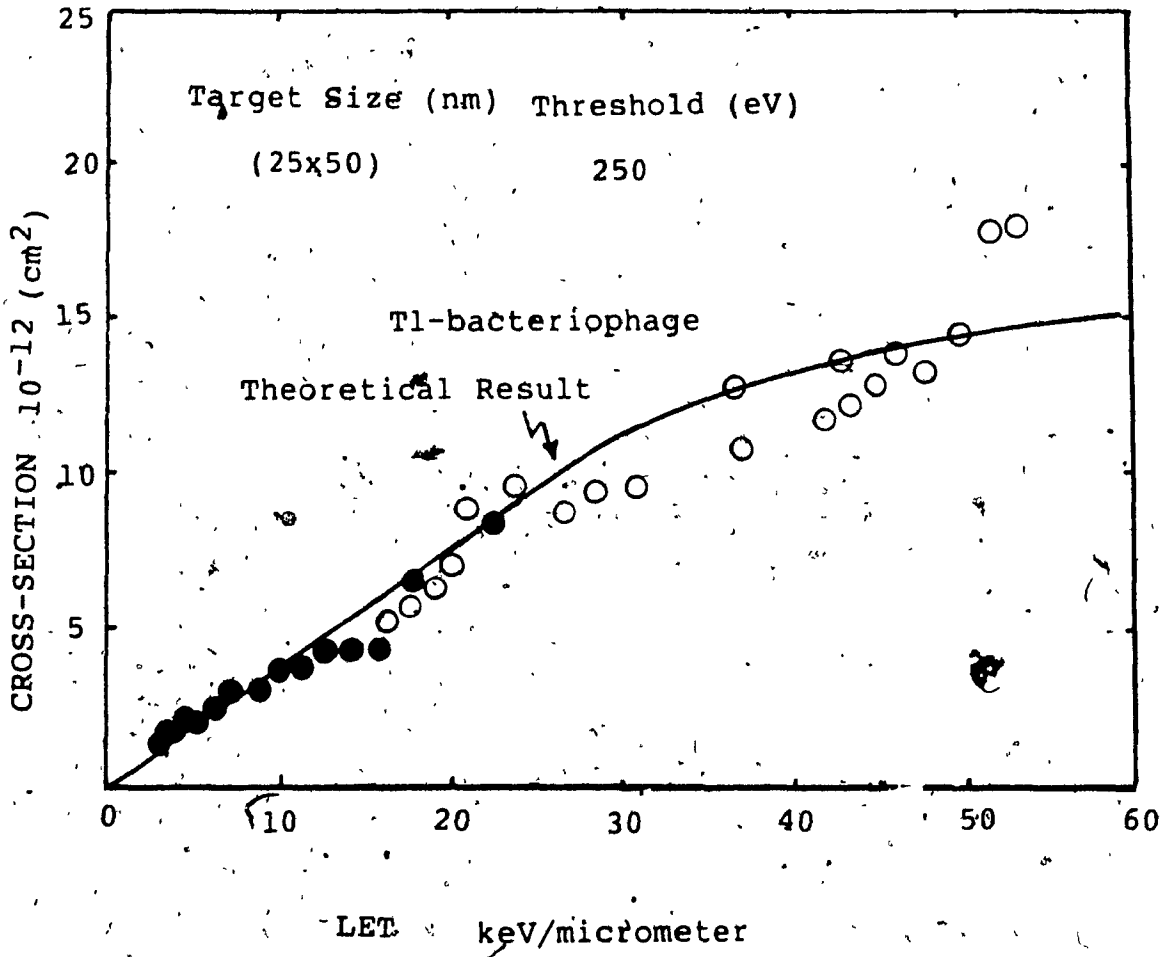

Fig.(5.9) Inactivation cross-section of Tl-bacteriophage by protons and alpha-particles against LET. Solid line represents theoretical values obtained by present work. The experimental results of Fluke and Forro (28) are shown as solid circles for protons and open circles for α-particles.

CHAPTER VI

Discussion and Conclusion

6.1 Discussion and Conclusion

The effects of heavy ions on biological systems have been discussed and the type of radiation effects were related to the target size or structure of the material in question. The list of radiation " molecular weights " given in Table I showed clearly that the technique of dry irradiation did not give values in agreement with those obtained by physico-chemical methods. Nonetheless, inactivation by radiation deserves a place with other physical methods of study because of the simplicity with which it gives better than order of magnitude results.

Katz's approach under the title of radial distribution of secondary ionization energy was discussed, and under this dose distribution the inactivation probability was related to the radial distance from the ion's path, and then integrated over all space to find inactivation cross-section.

A very different approach, the " Track Structure Theory ", which originally describes the spatial distribution of localized events was discussed. An attempt was made to assess how the frequency of event distribution was related to the inactivation cross-section. Variation in the nature of target sizes and relevant thresholds, in this calculation, were accounted for through the variation of the

probability. Calculations of cross-sections were made for various thresholds for cylinders of different length and diameter. The range of variation of the cross-sections for different target systems were calculated for different target sizes and tabulated in Appendix B.

Following computations of the inactivation cross-section, it was estimated that the volumes of targets vary with their sensitivity, for instance, the volume for insensitive materials, was 2x2, 3x3, ...nm^2 while it was 25x25, 50x50, ...nm^2 for sensitive materials.

However, the inactivation cross-sections have been calculated to produce a theoretical graph of σ versus LET using data based on the track simulation method. For insensitive materials, ${}_{\gamma}D^{37}=10^8$rad (according to the classification of Katz) reasonable agreement has been achieved in comparison with those of Katz Fig.(5.7). On the other hand, for sensitive materials, in the limit of LET<100 keV/micrometer the results of Katz (9) are simply consistent with our caculation, but for LET>100 keV/micrometer the deviation from Katz's results, becomes significant, that is, instead of sharp bends which is characteristic of the Katz results, we were confronted with a plateau in all cases Fig.(5.8). In spite of this small difference, the present model agrees substantially with the result of Katz.

Experimental verification of the calculations of the inactivation cross-sections, which was presented in section 5.6 constitutes an experimental verification of the model

used for the calculation.

Let us take a general view on the assumptions used in these two techniques. Katz assumes that the radiation flux throughout the system of interest is uniform and at a given distance from the track it is assumed that the target is subjected to the same dose and hence the same inactivation probability. This condition is difficult to meet. Since for very small volumes, say roughly 2x2 and 3x3 nm^2 many of the sampled volumes will contain no energy depositions, while a few will see many times the average. Therefore, the method of calculation is limited to average doses and fluctuations in dose cannot be taken into account.

On the other hand, Katz's calculation is rigorously valid only for point targets which can place limits on the expected validity of the results.

Also in Katz's approach, for simplicity in the calculation, electrons are assumed to be ejected normally to the ion's path. This assumption should introduce most serious error at low electron velocities. If the exact nature of electrons ejection is taken into account, the more energetic delta-rays are thrown forward, and σ is considerably smaller than shown in Katz's data.

Another oversimplification in Katz approach, arises from a range-energy formula for ejected electrons. This range-energy relation yields ranges below experimental practical ranges for electrons of higher energy (above 5 keV). For such electrons Katz's range-energy relationship

gives an energy loss rate which is too high.

Finally in all calculations, the delta-ray distribution formula which is used by Katz et al (9) is for free electrons. Errors arising from electron binding in the K-shell of oxygen may be expected to appear for inactivation cross-sections smaller than 10^{-12} cm^2.

Consquently, the essential difference between both strategies could be summarized as follows:

Katz's approach is an oversimplified of " Track Structure Theory " which neglects many basic facts in his calculations. Paretzke approach, on the other hand, tries directly to describe and predict the spatial distribution of localized events with a minimum of approximations and detailed analysis concerning preliminary physical processes, that is, specification of the nature of the activations and of their correlations are the main tasks in the " Track Structure Theory " of Paretzke. Thus, we expect this model to be a better solution for our problem than that of Katz.

Appendix A

Consider a target located with its " center of gravity " at distance x from the ion's path. Assume that target has m vital bonds at the distances x±yi from the ion's path, where i= 1,2,...,m/2. The probability of receiving one or more ionization is given by

$$P = 1 - \text{probablity of surviving} = 1 - \prod_{i=1}^{m/2} \exp\{-[D_\delta(x+yi)+D_\delta(x-yi)]/m_\gamma D^{37}\} =$$

$$1 - \exp-\{\sum_{i=1}^{m/2}[D_\delta(x+yi)+D_\delta(x-yi)]/m_\gamma D37\} \quad \text{(A.1)}$$

where $D_\delta(x\pm yi)$ is the local dose delivered by delta-rays at distance x±yi from the ion's path. By utilizing Eq.(5.8) we can have

$$D_\delta(x\pm yi) = Q\{(1/x^2)(1\pm yi/x)^{-2} - (1/xX)(1\pm yi/x)^{-1}\}$$

where $Q = [(8.5\times10^{-3})Z^*]/2\pi\beta^2]$

or

$$D_\delta(x+yi)+D_\delta(x-yi) = Q\{(2/x2)[1+3(yi/x)^2+...] - (2/xX)[1+(yi/x)^2+...]\} \quad \text{(A.2)}$$

For small values of yi/x this will simplified to

$$D_\delta(x+yi)+D_\delta(x-yi) \approx 2Q[(1/x^2) - (1/xX)] = 2D_\delta(x) \quad \text{(A.3)}$$

therefore, the probability of inactivation will be written as

$$1 - \exp\{-\sum_{i=1}^{m/2}[2D_\delta(x)/m_\gamma D^{37}]\} = 1 - \exp[-D_\delta(x)/ {}_\gamma D^{37}] \quad \text{(A.4)}$$

which is the expression that we have used.

APPENDIX B

The table headings give the particle energy and mean stopping power of the track.

The column headings are :

"Th"=Threshold (eV)

"D"=Diameter (nm)

"L"=Length (nm)

particle proton

Energy=4.00 MeV/amu

Average stopping power=8.8 keV/micrometer

TH	D	L	SIGMA
5	2	1.0	1.24E-14
16	2	2.0	1.24E-14
30	2	4.0	1.25E-14
50	2	8.0	1.19E-14
70	2	16.0	1.28E-14
28	3	1.5	1.26E-14
50	3	3.0	1.27E-14
72	3	6.0	1.25E-14
106	3	12.0	1.22E-14
148	3	24.0	1.23E-14
50	4	2.0	1.24E-14
80	4	4.0	1.25E-14
120	4	8.0	1.26E-14
170	4	16.0	1.24E-14
230	4	32.0	1.21E-14
80	5	2.5	1.26E-14
125	5	5.0	1.22E-14
180	5	10.0	1.24E-14
250	5	20.0	1.22E-14
307	5	40.0	1.22E-14
150	7	3.5	1.17E-14
212	7	7.0	1.30E-14
300	7	14.0	1.26E-14
400	7	28.0	1.20E-14
260	10	5.0	1.28E-14
370	10	10.0	1.23E-14
520	10	20.0	1.19E-14

Energy=2.00 MeV/amu

Average stopping power=16.0 keV/ micrometer

TH	D	L	SIGMA
5	2	1.0	1.94E-14
16	2	2.0	2.29E-14
30	2	4.0	2.14E-14
50	2	8.0	2.21E-14
70	2	16.0	2.47E-14
28	3	1.5	2.19E-14
50	3	3.0	1.98E-14
72	3	6.0	2.38E-14
106	3	12.0	2.53E-14
148	3	24.0	2.46E-14
50	4	2.0	2.37E-14
80	4	4.0	2.56E-14
120	4	8.0	2.84E-14
170	4	16.0	2.82E-14
230	4	32.0	2.44E-14
80	5	2.5	2.47E-14
125	5	5.0	2.59E-14
180	5	10.0	2.72E-14
250	5	20.0	2.74E-14
307	5	40.0	2.95E-14
150	7	3.5	2.63E-14
212	7	7.0	3.08E-14
300	7	14.0	3.02E-14
400	7	28.0	2.87E-14
260	10	5.0	2.96E-14
370	10	10.0	2.93E-14
520	10	20.0	2.57E-14

particle proton

Energy=1.00 MeV/amu Energy=.50 MeV/amu

Average stopping power=25.8 keV/micrometer Average stopping power =40.1 keV/micrometer

TH	D	L	SIGMA
5	2	1.0	2.93E-14
16	2	2.0	3.54E-14
30	2	4.0	3.75E-14
50	2	8.0	4.14E-14
70	2	16.0	4.90E-14
28	3	1.5	3.47E-14
50	3	3.0	3.70E-14
72	3	6.0	4.79E-14
106	3	12.0	5.28E-14
148	3	24.0	5.19E-14
50	4	2.0	4.54E-14
80	4	4.0	5.23E-14
120	4	8.0	5.96E-14
170	4	16.0	6.31E-14
230	4	32.0	5.97E-14
80	5	2.5	5.25E-14
125	5	5.0	5.67E-14
180	5	10.0	6.34E-14
250	5	20.0	6.25E-14
307	5	40.0	7.29E-14
150	7	3.5	6.00E-14
212	7	7.0	8.05E-14
300	7	14.0	7.88E-14
400	7	28.0	8.43E-14
260	10	5.0	7.64E-14
370	10	10.0	8.82E-14
520	10	20.0	8.82E-14

TH	D	L	SIGMA
5	2	1.0	4.20E-14
16	2	2.0	5.06E-14
30	2	4.0	5.82E-14
50	2	8.0	6.95E-14
70	2	16.0	9.21E-14
28	3	1.5	5.32E-14
50	3	3.0	6.19E-14
72	3	6.0	8.57E-14
106	3	12.0	1.06E-13
148	3	24.0	1.19E-13
50	4	2.0	7.42E-14
80	4	4.0	9.39E-14
120	4	8.0	1.18E-13
170	4	16.0	1.42E-13
230	4	32.0	1.57E-13
80	5	2.5	9.16E-14
125	5	5.0	1.13E-13
180	5	10.0	1.71E-13
250	5	20.0	1.67E-13
307	5	40.0	2.07E-13
150	7	3.5	1.24E-13
212	7	7.0	1.80E-13
300	7	14.0	2.07E-13
400	7	28.0	2.36E-13
260	10	5.0	2.03E-13
370	10	10.0	2.61E-13
520	10	20.0	2.85E-13

particle; proton

Energy=.30 MeV/amu

Average stopping power=58.9 keV/micrometer

TH	D	L	SIGMA
5	2	1.0	5.51E-14
16	2	2.0	6.65E-14
30	2	4.0	8.07E-14
50	2	8.0	1.09E-13
70	2	16.0	1.56E-13
28	3	1.5	7.75E-14
50	3	3.0	9.03E-14
72	3	6.0	1.31E-13
106	3	12.0	1.81E-13
148	3	24.0	2.36E-13
50	4	2.0	1.07E-13
80	4	4.0	1.43E-13
120	4	8.0	1.96E-13
170	4	16.0	2.69E-13
230	4	32.0	3.43E-13
80	5	2.5	1.42E-13
125	5	5.0	1.86E-13
180	5	10.0	2.57E-13
250	5	20.0	3.43E-13
307	5	40.0	5.02E-13
150	7	3.5	2.11E-13
212	7	7.0	3.17E-13
300	7	14.0	4.27E-13
400	7	28.0	5.59E-13
260	10	5.0	3.64E-13
370	10	10.0	5.49E-13
520	10	20.0	6.91E-13

Paticle; Alpha

Energy=1.50 MeV/amu

Average stopp ing power=73.7 keV/micrometer

TH	D	L	SIGMA
5	2	1.0	6.82E-14
16	2	2.0	8.11E-14
30	2	4.0	9.75E-14
50	2	8.0	1.29E-13
70	2	16.0	1.86E-13
28	3	1.5	8.01E-14
50	3	3.0	1.07E-13
72	3	6.0	1.54E-13
106	3	12.0	2.16E-13
148	3	24.0	2.79E-13
50	4	2.0	1.29E-13
80	4	4.0	1.69E-13
120	4	8.0	2.29E-13
170	4	16.0	3.21E-13
230	4	32.0	4.12E-13
80	5	2.5	1.65E-13
125	5	5.0	2.18E-13
180	5	10.0	3.06E-13
250	5	20.0	4.10E-13
307	5	40.0	6.01E-13
150	7	3.5	2.54E-13
212	7	7.0	3.69E-13
300	7	14.0	5.05E-13
400	7	28.0	6.70E-13
260	10	5.0	4.41E-13
370	10	10.0	6.29E-13
520	10	20.0	8.30E-13

Particle; Alpha

Energy=1.00 MeV/amu

Average stopping power=102.5 keV/micrometer

TH	D	L	SIGMA
5	2	1.0	8.81E-14
16	2	2.0	1.05E-13
30	2	4.0	1.30E-13
50	2	8.0	1.68E-13
70	2	16.0	2.56E-13
28	3	1.5	1.16E-13
50	3	3.0	1.39E-13
72	3	6.0	2.04E-13
106	3	12.0	2.94E-13
148	3	24.0	4.28E-13
50	4	2.0	1.62E-13
80	4	4.0	2.16E-13
120	4	8.0	3.08E-13
170	4	16.0	4.61E-13
230	4	32.0	6.21E-13
80	5	2.5	2.16E-13
125	5	5.0	2.88E-13
180	5	10.0	4.20E-13
250	5	20.0	6.22E-13
307	5	40.0	9.96E-13
150	7	3.5	3.43E-13
212	7	7.0	4.96E-13
300	7	14.0	7.17E-13
400	7	28.0	1.09E-12
260	10	5.0	6.13E-13
370	10	10.0	8.84E-13
520	10	20.0	1.29E-12

Energy=.75 MeV/amu

Average stopping power=129.9 keV/micrometer

TH	D	L	SIGMA
5	2	1.0	9.85E-14
16	2	2.0	1.17E-13
30	2	4.0	1.32E-13
50	2	8.0	2.01E-13
70	2	16.0	3.13E-13
28	3	1.5	1.30E-13
50	3	3.0	1.57E-13
72	3	6.0	2.30E-13
106	3	12.0	3.47E-13
148	3	24.0	5.35E-13
50	4	2.0	1.85E-13
80	4	4.0	2.44E-13
120	4	8.0	3.50E-13
170	4	16.0	5.46E-13
230	4	32.0	8.53E-13
80	5	2.5	2.43E-13
125	5	5.0	3.25E-13
180	5	10.0	4.81E-13
250	5	20.0	7.55E-13
307	5	40.0	1.27E-12
150	7	3.5	3.92E-13
212	7	7.0	5.59E-13
300	7	14.0	8.42E-13
400	7	28.0	1.38E-12
260	10	5.0	7.07E-13
370	10	10.0	1.01E-12
520	10	20.0	1.54E-12

Particle; Alpha

Energy=.50 MeV/amu

Average stopping power=167.2 keV/micrometer

TH	D	L	SIGMA
5	2	1.0	1.13E-13
16	2	2.0	1.30E-13
30	2	4.0	1.65E-13
50	2	8.0	2.32E-13
70	2	16.0	3.66E-13
28	3	1.5	1.51E-13
50	3	3.0	1.81E-13
72	3	6.0	2.76E-13
106	3	12.0	4.09E-13
148	3	24.0	6.43E-13
50	4	2.0	2.13E-13
80	4	4.0	2.81E-13
120	4	8.0	4.09E-13
170	4	16.0	6.44E-13
230	4	32.0	1.07E-12
80	5	2.5	2.86E-13
125	5	5.0	3.74E-13
180	5	10.0	5.62E-13
250	5	20.0	8.91E-13
307	5	40.0	1.58E-12
150	7	3.5	4.53E-13
212	7	7.0	6.39E-13
300	7	14.0	9.69E-13
400	7	28.0	1.65E-12
260	10	5.0	8.45E-13
370	10	10.0	1.15E-12
520	10	20.0	1.81E-12

Energy=.30 MeV/amu

Average stopping power=230.1 keV/micrometer

TH	D	L	SIGMA
5	2	1.0	1.31E-13
16	2	2.0	1.57E-13
30	2	4.0	1.94E-13
50	2	8.0	2.71E-13
70	2	16.0	4.34E-13
28	3	1.5	1.76E-13
50	3	3.0	2.08E-13
72	3	6.0	3.01E-13
106	3	12.0	4.57E-13
148	3	24.0	7.47E-13
50	4	2.0	2.38E-13
80	4	4.0	3.07E-13
120	4	8.0	4.39E-13
170	4	16.0	6.98E-13
230	4	32.0	1.20E-12
80	5	2.5	3.18E-13
125	5	5.0	4.06E-13
180	5	10.0	5.95E-13
250	5	20.0	9.80E-13
307	5	40.0	1.75E-12
150	7	3.5	4.83E-13
212	7	7.0	6.73E-13
300	7	14.0	1.04E-12
400	7	28.0	1.76E-12
260	10	5.0	8.63E-13
370	10	10.0	1.21E-12
520	10	20.0	1.93E-12

APPENDIX C

LISTING OF COMPUTER PROGRAM

```
      PROGRAM COMP( INPUT,OUTPUT,TAPE1 )
      REAL L
      INTEGER Th, D, C
      XL=8.8
      PRINT*, '*******************************'
      PRINT*, 'Th      D      L      SIGMA'
      C=1
      DO  35  I=1, 27
      READ (1,*)P,Th,D,L
      IF(D.NE.C)Then
      PRINT*, '*******************************'
      END IF
      SIGMA=16*XL*P*10**(-17.)
      PRINT* 100,Th,D,L,SIGMA
100   FORMAT(I4,3X,I2,3X,F4.1,3X,E9.3)
      C=D
35    CONTINUE
      PRINT*, '*******************************'
      PRINT*, '*******************************'
      STOP
      END
```

REFERENCES

1. R. G. Hussey and W. R. Thompson; J. Gen. Physiol. 5(1923)674.

2. J. H. Northrop, J. Gen. Physiol. 17(1934)359.

3. H. Frick, Cold Spring Harbor Symp. 2(1934)241.

3a. T. Svedberg and S. Brohult, Nature 1(1934)143.

4a. D. E. Lea, K. M. Smith, B. Holmes, and R. Markham, Parasitology, 36(1944) 110.

4b. D. E. Lea, " Action of Radiations on Living Cells ", University press, Combridge, 1962.

5a. E. C. Pollard, A. Buzzell, C. Jeffreys and F. Forro, Jr. Biochem. Biophys. 33(1951)9.

5b. E. C. Pollard, W. R. Guild, F. Hutchinson, and R. B. Setlow, Progr. Biophys. 5(1955)108.

5c. E. C. Pollard, Am. Scientist, 39(1951)99.

5d. E. C. Pollard, " The Physics of Viruses ", Academic Press, New York, 1953.

6a. T. Brustad, Rad. Res. 15(1961)139.

6b. T. Brustad, Rad. Res. Supplementary 7, 74(1967)74.

7. P. Alexander, Rad. Res. 6(1957)653.

8. G. W. Dolphin and F. Hutchinson, Rad. Res. 13(1960)403.

9a. R. Katz, S. C. Sharma, M. Homayoonfar, The Structure of Particle Tracks, in " Topics in Radiation Dosimetry ", Radiation Dosimetry Supplementary I, F. H. Attix C. William Roesh and Tochilin (Eds.), Academic Press,

New YorK, 1972.

9b. J. J. Butts, and R. Katz, Rad. Res. 30(1971)855.

10a. H. G. Paretzke, Advances in Energy Deposition Theory, in " Advances in Radiation Protection and Dosimetry ", R. H. Thomas and V. Perez-Mendez (Eds.), Plenum Press, New York, 1980.

10b. H. G. Paretzke, " Radiation Track Structure Theory ", G. R. Freeman (Ed.), in " Kinetics of Nonhomogeneous Processes ", G. R. Freeman (Ed.), John Wiley and Sons, Inc. New York, 1987.

10c. H. G. Paretzke, On Limitations of Classical Microdosimetry and Advantages of Track Structure Analysis for Radiation Biology, in Sixth Symposium on Microdosimetry, J. Booz and E. G. Ebert (Eds.), Harwood Academic Publishers Ltd. Brussels, 1979.

11. D. E. Charlton, D. T. Goodhead, W. E. Wilson, and H. G. Paretzke, " Energy Deposition in Cylindrical Volumes ", Medical Research Council, Radiobiology Unit, Chilton, 1985.

12. Ulrey in H. Semat, " Introduction to Atomic and Nuclear Physics ", H. Rinhat and Winston (Eds.), New York, 1972.

13. I. Kaplan, " Nuclear Physics ", Addison-Wesley, New York, 1966.

14. R. T. Weinder and R. L. Sells, " Elementary Modern Physics ", Allyn and Bacon, New York, 1980.

15. R. Raja, J. T. Lyman, T. Brustad, and C. A.

Tobias, Heavy Charged Particle Beams in Radiation Dosimetry, III, F. H. Attix C. William, (Eds.), Academic Press, New York, 1969.

16. J. Neufeld, W. S. Synder, " Selected Topics in Radiation Dosimetry ", Vienna, Inter. Atom. Energy, 35,1961.

17. F. Bloch, " Lecture Series in Nuclear Physics ", MDDC-1175, U. S. Government Publishing House, 1947.

18. J. D. Jackson, " Classical Electrodynamics ", Wiley, New York, 1975.

19. J. Hale, " The Fundamentals of Radiological Science ", Springfield, Illinois, Thomas (Ed.), 1974.

20. H. H. Rossi, Microdosimetry and Radiobiology, in " Radiation Protection Dosimetry ", Nuclear Technology Publishing, Vol.13 No. 1-4 P. 254-256, 1985.

21a. W. K. Sinclair, Radiobiological Dosimetry, in " Radiation Dosimetry III ", F. H. Attix, C. William, R. Tochilin (Eds.), Academic Press, New York, 1969.

21b. W. K. Sinclair, The Shape of Radiation Survival Curves of Mammalian Cells Cultured in Vitro, Tech. Rep. Ser. No. 58, Vienna, 1966.

22. A. Kellerer, Dose Effect Relation and the Inactivation of Absorption events, Tech. Rep. Ser. No. 58, Vienna, 1966.

23. H. Dertinger and H. Jung, " Molecular Radiation Biology ",Translated by R. B. Huber and P. A. Gresham, Springer Verlag (Ed.), New York, 1970.

24. R. B. Setlow, Arch. Biochem. Biophys. 36(1952)328.

25. H. Barkas, " Nuclear Research Emulsions ", Academic Press, New York, 1963.

26. I. M. Sobol, " The Monte Carlo Method ", Translated by V. I. Kisin, Mir. Publishers, Moscow, 1984.

27. D. T. Goodhead, R. J. Munson, J. Thacker, and R. Cox, Int. J. Rad. Biol. 37(1980)135.

28. D. J. Fluke and F. Forro, Rad. Res. 13(1960)305.

29. N. Bohr, " Penetration of Atomic Particles through Matter ", Kgl. Danske Videnskab. Selskab Mat.-fse. Medd. XVIII, No. 8, 1948.